Deep learning-based Alzheimer's disease diagnostics using medical images

by

Mohammad Seraj

Under the supervision
of
Dr N Arul Murugan
Dr AV Subramaniyam

Indraprastha Institute of Information Technology Delhi
May, 2024

Deep learning-based Alzheimer's disease diagnostics using medical images

by

Mohammad Seraj

Submitted
in partial fulfilment of the requirements for the degree of
Master of Technology

to

Indraprastha Institute of Information Technology Delhi
May, 2024

Certificate

This is to certify that the thesis titled **"Deep learning-based Alzheimer's disease diagnostics using medical images"** being submitted by **Mohammad Seraj** to the Indraprastha Institute of Information Technology Delhi, for the award of the Master of Technology, is an original research work carried out by him under my supervision. In my opinion, the thesis has reached the standards fulfilling the requirements of the regulations relating to the degree.

The results contained in this thesis have not been submitted in part or full to any other university or institute for the award of any degree/diploma.

May, 2024

Dr. N Arul Murugan
Department of Computational Biology
Indraprastha Institute of Information Technology
Delhi, New Delhi 110020

Dr AV Subramaniyam
Department of Electronics & Communications Engineering
Indraprastha Institute of Information Technology
Delhi, New Delhi 110020

Acknowledgements

I am sincerely grateful to Dr. N Arul Murugan, my thesis supervisor, and Dr. AV Subramaniyam, my co-supervisor, for their invaluable mentorship and unwavering support throughout this endeavor. Their expertise and encouragement played a pivotal role in the successful completion of this thesis. I am also indebted to all the faculty and staff at IIIT Delhi for their consistent assistance, which greatly facilitated the entire process. Thank you all for your guidance and support.

I am indebted to my fellow batchmates for their encouragement and support, and I wish to express particular thanks to Prateek Paul from the Ph.D. 2022 batch for his significant contribution to this work.

Lastly, heartfelt thanks are extended to my family, whose enduring support and inspiration have been pivotal throughout my academic journey. Their unwavering belief in me has made this achievement possible.

Abstract

In the ever-evolving landscape of medical innovation, the pursuit of accurate and efficient diagnostic tools for neurodegenerative diseases, notably Alzheimer's, has become increasingly urgent. The relentless progression of medical imaging technology, particularly magnetic resonance imaging (MRI), has sparked a wave of research aimed at harnessing advanced computational techniques, such as deep learning, to enhance diagnostic accuracy and efficiency. This thesis delves into the exploration of innovative deep-learning methodologies tailored specifically for Alzheimer's disease diagnosis based on MRI data, with a focus on three distinct sections of the brain: Sagittal, Axial, and Coronal. The research journey begins with the development of a 2D slice-based convolutional neural network (CNN) model, meticulously designed to analyze MRI scans in each section individually. Notably, the Sagittal section achieves an accuracy of 44%, the Axial section achieves 47%, and the Coronal section achieves 48%. As the study progresses, attention turns towards the utilization of 3D CNNs, a more holistic approach capable of processing MRI volumes as three-dimensional entities. This model, accommodating the depth of MRI data, presents a novel perspective on Alzheimer's disease diagnosis, capturing intricate spatial relationships within the brain. However, despite its promise, the 3D CNN model exhibits varying degrees of accuracy across different sections, with an overall accuracy of 60%. Furthermore, the research delves into the exploration of a patch-based classification model, aiming to enhance diagnostic accuracy through a localized analysis of MRI data. By dividing MRI volumes into smaller patches and classifying each patch individually, this approach offers a fine-grained understanding of pathological changes associated with Alzheimer's disease. However, despite its potential, the patch-based model demonstrates challenges in achieving comparable accuracy to its slice-based counterparts, with an overall accuracy of 52%. Moreover, the evaluation of these models reveals intriguing insights into the strengths and limitations of different approaches. The study explores both slice-based 2D CNN and 3D CNN approaches for MRI analysis. In the 3D CNN approach, the MRI volumes are resized to a uniform shape, accommodating variations in MRI depth across different datasets. This diverse dataset facilitates the development of models capable of accurately distinguishing between different disease stages, thereby aiding in early diagnosis and personalized treatment planning.

In conclusion, this thesis contributes to the burgeoning field of medical image analysis by presenting innovative deep learning approaches tailored for Alzheimer's disease diagnostics. Through the integration of advanced algorithms and comprehensive evaluation, this research paves the way for more reliable and efficient diagnostic tools, ultimately leading to improved patient outcomes and healthcare management in neurodegenerative disease.

Keywords: Alzheimer’s disease,CNN,MRI, Axial, Coronal, Sagittal

Contents

1 Introduction..... 1
1.1 Alzheimer's Disease and Its Stages..... 1
1.2 Understanding MRI: Insights into Brain Imaging..... 2
1.3 T1-Weighted MRI..... 2
1.4 CNN Based Alzheimer's Disease Diagnosis..... 2
2 Literature Review..... 3
3 Materials and Methods..... 4
3.1 Dependencies Installation..... 4
3.2 Data Collection..... 5
3.3 Data Sorting: Organization into Class Categories..... 5
3.4 Deciphering Complexity: Navigating Exploratory Data Analysis..... 6
3.5 Work – Flow..... 8
3.6 Skull Stripping with ANTsPyNet Library: An Efficient Approach for Brain Image Processing..... 9
3.7.1 Exploring the Critical Terminology of MRI: Orientation and Voxel Arrangement..... 10
3.7.2 ANTsPyNet Approach to Brain Extraction Procedure..... 13
4 Deep Learning-Based Framework for Disease Prediction from MRI Data: Methodology and Performance Analysis..... 14
4.1.1 Deep Learning Approach for Disease Detection in MRI Images: A 2D CNN – Slice Based Model Training for multiclass classification..... 14
4.1.1.2 Data split Explanation for the 2D CNN slice based model..... 15
4.1.2 Data Pre-processing for Sagittal Section..... 16
4.1.3 Data Pre-processing for Axial Section..... 17
4.1.4 Data Pre-processing for Coronal Section..... 18
4.1.5 Architecture overview for 2D slice-based classification..... 19
4.1.5.1 Model Architecture Strategies for Sagittal Section of 2D CNN..... 20
4.1.5.2 Model Architecture Strategies for Axial Section of 2D CNN..... 20
4.1.5.3 Model Architecture Strategies for Coronal Section of 2D CNN..... 21
4.2 Empowering Alzheimer's Disease Classification in MRI via 3D CNN-based Models..... 22
4.2.1 Overview..... 22
4.2.2 Preparation of Data for Training the 3D CNN Model..... 23
4.2.3 Architecture Overview..... 24
4.3 Alzheimer's Disease Detection via Patch-Based Convolutional Neural Networks..... 25
4.3.1 Overview..... 25
4.3.2 Data Pre-process for the patch-based CNN..... 25
4.3.3 Model Architecture..... 26
5 Result and Discussion..... 28
5.1 Sagittal section 2D slices-based model outcomes..... 28
5.2 Axial section 2d slices-based model outcomes..... 30
5.3 Coronal section 2d slices-based model outcomes..... 33
5.4 3D CNN-based Model Outcomes..... 36
5.5 Patch-Based Convolutional Neural Networks..... 37

5.7 Discussion..... 40
5.8 Future Scope..... 40
6 Conclusion..... 41
References..... 42

List of Figures

Figure:1.1 Increasing order of disease severity..... 1
Figure 3.3.1 Data sorting on the basis of their group..... 5
Figure:3.4.1 Histogram shows the counts of different classes..... 6
Figure:3.4.2 Pie-chart shows count of male and female MRI data..... 6
Figure:3.4.3 Heatmap show counts Alzheimer disease stage in various age groups..... 7
Figure:3.4.4 Bar graph show counts Alzheimer disease stage in various 7
Figure:3.5.1 A structured workflow from data collection to model training..... 8
Figure:3.6.1 The ANTsRNet and ANTsPyNet deep learning toolkits..... 9
Figure:3.7.2.1 Brain extraction procedure..... 13
Figure:4.1.1 Distribution of Alzheimer's MRI Data for Model Training with Class Assignments for 2D CNN..... 15
Figure:4.1.2 Distribution of Alzheimer's MRI Data for Model Validation with Class Assignments for 2D CNN..... 15
Figure:4.1.2.1 Visualization of Sagittal Section MRI samples depicting different stages of Alzheimer's Disease. From top: Sample of AD (Alzheimer's Disease), CN (Cognitive Normal), EMCI (Early Mild Cognitive Impairment)..... 16
Figure:4.1.2.2 Visualization of Sagittal Section MRI samples depicting different stages of Alzheimer's Disease. From top: Sample of LMCI (Late Mild Cognitive Impairment), MCI (Mild Cognitive Impairment), SMC (Subjective Memory Complaints)..... 16
Figure:4.1.3.1 Visualization of Axial Section MRI samples depicting different stages of Alzheimer's Disease. From top: Sample of AD (Alzheimer's Disease), CN (Cognitive Normal), EMCI (Early Mild Cognitive Impairment)..... 17
Figure:4.1.3.2 Visualization of Axial Section MRI samples depicting different stages of Alzheimer's Disease. From top: Sample of LMCI (Late Mild Cognitive Impairment), MCI (Mild Cognitive Impairment), SMC (Subjective Memory Complaints)..... 17
Figure:4.1.4.1 Visualization of Coronal Section MRI samples depicting different stages of Alzheimer's Disease. From top: Sample of AD (Alzheimer's Disease), CN (Cognitive Normal), EMCI (Early Mild Cognitive Impairment)..... 17

Figure:4.1.4.1 Visualization of Coronal Section MRI samples depicting different stages of Alzheimer's Disease. From top: Sample of AD (Alzheimer's Disease), CN (Cognitive Normal), EMCI (Early Mild Cognitive Impairment)..... 18
Figure:4.1.4.2 Visualization of Coronal Section MRI samples depicting different stages of Alzheimer's Disease. From top: Sample of LMCI (Late Mild Cognitive Impairment), MCI (Mild Cognitive Impairment), SMC (Subjective Memory Complaints)..... 18
Figure:4.1.5.1 CNN based model architecture for sagittal section of the brain..... 20
Figure:4.1.6.1 CNN based model architecture for axial section of the brain..... 20
Figure:4.1.7.1 CNN based model architecture for coronal section of the brain..... 21
Figure:4.2.1.1 Distribution of Alzheimer's MRI Data for Model Training with Class Assignments..... 22
Figure:4.2.1.2 Distribution of Alzheimer's MRI Data for Model Validation with Class Assignments..... 22
Figure:4.2.2.1 Visualization of MRI data used for the 3D CNN..... 23
Figure: 4.2.3.1 Implementation of a 3D-CNN model for the purpose of multiclass classification..... 24
Figure: 4.3.3.1 Developing a ResNet-18 implementation tailored for training a patch-based model for multiclass classification..... 27
Figure:5.1.1 Model Accuracy vs Epoch of Sagittal Section..... 28
Figure:5.1.2 Model Loss of Sagittal Section..... 28
Figure:5.1.3 Sagittal Section Confusion Matrix..... 29
Figure:5.1.4 Prediction on test sample: The prediction result suggest that person is AD: Alzheimer Disease 30
Figure:5.2.1 Model Accuracy vs Epoch of Axial Section..... 30
Figure:5.2.2 Model Loss of Axial Section..... 31
Figure:5.2.3 Confusion Matrix of Axial Section..... 32
Figure:5.2.4 Prediction on test sample: The prediction result suggest that person is suffering from AD: Alzheimer Disease..... 32
Figure:5.3.1 Model Accuracy vs Epoch of Coronal Section..... 33
Figure:5.3.2 Model Loss of Coronal Section..... 33
Figure:5.3.3. Confusion Matrix of Coronal Section..... 34
Figure: 5.3.4 Prediction on test sample: The prediction result suggest that person is suffering from Early Mild Cognitive Impairment..... 35

Figure:5.4.1 Model loss vs Epoch of 3D MRI..... 36
Figure:5.4.2 Model Accuracy vs Epoch of 3D MRI..... 36
Figure:5.5.1 Model Training and Validation Accuracy and Loss..... 37
Figure:5.5.2 Patch-Based Convolutional Neural Networks Model Confusion Matrix..... 38
Figure:5.5.3 Prediction on test sample: The prediction result suggest that person is suffering from Early Mild Cognitive Impairment (EMCI)..... 39

List of Tables

Table:5.1.1 Sagittal Section Classification Report..... 29
Table:5.2.1 Axial Section Classification Report..... 31
Table:5.3.1 Coronal Section Classification Report..... 34
Table:5.3.1 Performance Evaluation Matrix Across Three Brain MRI Sections for Validation of 2D CNN Model..... 35
Table:5.5.1 Patch-Based Convolutional Neural Networks Classification Report..... 37

Chapter 1

1 Introduction

1.1 Alzheimer's Disease and Its Stages

In the landscape of medical diagnostics, the integration of deep learning methodologies with medical imaging data represents a promising avenue for enhancing precision and efficacy in disease detection and classification. Among the myriad of medical conditions necessitating accurate diagnosis, Alzheimer's disease poses a formidable challenge. Characterized by progressive cognitive decline and neurodegeneration, Alzheimer's disease not only imposes significant burdens on affected individuals and their families but also presents substantial challenges to healthcare systems worldwide.

The focus of this thesis lies in exploring the potential of deep learning-based approaches for the detection of Alzheimer's disease using medical imaging data, with magnetic resonance imaging (MRI) serving as the primary modality. Specifically, the research endeavours to develop and evaluate deep learning models tailored for the detection and classification of Alzheimer's disease based on MRI scans.

A crucial aspect of this research involves the utilization of a dataset encompassing six stages of Alzheimer's disease progression, as delineated by the Alzheimer's Disease Neuroimaging Initiative (ADNI). These stages include:

1. **Alzheimer's Disease (AD):** Characterized by significant cognitive decline and impairment in daily functioning, Alzheimer's disease represents the advanced stage of neurodegeneration.
2. **Cognitive Normal (CN):** Individuals classified as cognitive normal exhibit no discernible cognitive impairment and serve as a reference group for comparison.
3. **Mild Cognitive Impairment (MCI):** Marked by noticeable cognitive decline beyond what is expected for age, mild cognitive impairment represents an intermediate stage between normal aging and dementia.
4. **Early Mild Cognitive Impairment (EMCI):** Referring to the initial stages of cognitive impairment, early mild cognitive impairment represents a subtle decline in cognitive function that may progress to more severe impairment over time.
5. **Late Mild Cognitive Impairment (LMCI):** Reflecting a more advanced stage of cognitive impairment, late mild cognitive impairment denotes a further deterioration in cognitive function, often accompanied by increased functional impairment.
6. **Subjective Memory Complaints (SMC)**: Represent subjective memory complaints observed in individuals, indicating potential early signs of cognitive decline. These complaints manifest as self-reported memory difficulties or cognitive lapses, prompting further investigation. Including individuals with SMC enriches the dataset diversity, facilitating the exploration of subtle differences in MRI scans associated with early Alzheimer's disease progression.

Figure:1.1Increasing order of disease severity [1]

1.2 Understanding MRI: Insights into Brain Imaging

Magnetic Resonance Imaging (MRI) is pivotal for its detailed visualization of brain structures, revealing anomalies like tumours and atrophy. Beyond static imaging, techniques like functional MRI (fMRI) track blood flow changes, mapping neural activity during tasks[2]. Diffusion Tensor Imaging (DTI) traces water molecule diffusion along nerve fibres, elucidating white matter tracts and brain connectivity. These methods unveil brain function and pathology, aiding in neurological disorder research and patient care. They contribute to understanding cognitive processes, language, memory, and emotion, advancing medical science. MRI's versatility extends to studying aging and disease impacts on the brain, improving diagnosis and treatment [3].

1.3 T1-Weighted MRI

T1-weighted MRI (Magnetic Resonance Imaging) is a widely used imaging technique in medical diagnostics, particularly for visualizing anatomical structures within the body, including the brain. The "T1" designation in T1-weighted refers to the longitudinal or spin-lattice relaxation time of hydrogen nuclei in tissues, which is a fundamental property measured during MRI scans. T1-weighted images are created by assessing the signal intensity of tissues based on their T1 relaxation times. In T1-weighted MRI images, different tissues exhibit distinct signal intensities, enabling clear differentiation between structures. Typically, cerebrospinal fluid (CSF) appears dark, gray matter appears as medium gray, and white matter appears brighter. This inherent contrast facilitates the identification and assessment of various anatomical features and abnormalities within the brain. T1-weighted MRI is a crucial tool in clinical diagnosis, providing detailed structural information essential for detecting abnormalities such as tumors, ischemic lesions, hemorrhages, and atrophy. Moreover, it serves as a baseline for longitudinal studies, enabling the monitoring of changes in brain structure over time, particularly in conditions like Alzheimer's disease and other neurodegenerative disorders [4].

1.4 CNN Based Alzheimer’s Disease Diagnosis

CNN-based Alzheimer's disease diagnosis represents a significant advancement in medical research, particularly in the field of medical imaging analysis. Convolutional neural networks (CNNs) stand out as artificial intelligence algorithms inspired by the intricate workings of the human brain. Their remarkable ability to discern patterns and features within images makes them invaluable for deciphering complex medical scans such as MRI and CT images. In the realm of CNNs, 2D CNNs specialize in scrutinizing images along two dimensions, typically height and width. They employ filters across these dimensions to detect crucial features like edges, textures, and shapes. As a result, 2D CNNs excel in tasks such as image classification and object detection.
In contrast, 3D CNNs build upon this foundation by incorporating depth into their analysis. This extension enables them to handle volumetric data, such as medical scans, which contain information across three dimensions: height, width, and depth. Leveraging this capability, 3D CNNs can capture spatial relationships more effectively, proving advantageous for tasks demanding a nuanced understanding of the structure and context within volumetric data, such as medical diagnosis and segmentation [5].

Chapter 2

Literature Review

Alzheimer's disease (AD) presents a significant global health challenge, with its prevalence expected to rise as populations age. Early and accurate diagnosis is crucial for effective management and intervention. Recent advancements in machine learning (ML) and artificial intelligence (AI) have opened new avenues for improving AD diagnosis through the analysis of medical imaging data and clinical variables. Several studies have explored various ML techniques to enhance diagnostic accuracy, prognosis, and understanding of disease progression.One notable study compared the performance of two deep learning models, DenseNet-169 and ResNet-50, in diagnosing Alzheimer's disease [6]. The study found that DenseNet-169 achieved higher accuracy values during both training and testing phases compared to ResNet-50. This indicates that the architecture of DenseNet-169 may be better suited for capturing the intricate patterns present in AD-related data. Moreover, the study highlighted the importance of addressing data scarcity in AD research. To overcome this challenge, generative modelling techniques were employed to generate realistic brain images, thereby enhancing the robustness and generalizability of machine learning models for improved diagnosis.

Another innovative approach involved trajectory modelling to forecast future cognitive decline in AD patients using baseline data [7]. By training on "noisy" diagnostic labels, this method generated continuous prognostic scores for cognitive decline, leading to enhanced model accuracy. The trajectory modelling approach captured individual disease paths, reducing misclassification risks and enabling more precise predictions of AD progression. This method showcased the potential of leveraging machine learning techniques to extract crucial data structures and improve our understanding of disease trajectories in Alzheimer's.

In the realm of medical imaging, Vision Transformer (ViT) technology has been employed to analyze Magnetic Resonance Images (MRIs) for AD diagnosis [8]. ViT utilizes sequence modelling to maintain interdependencies in data and employs a time series transformer for classification. Evaluation using ADNI T1-weighted MRIs demonstrated promising results, with high accuracy rates achieved for both binary and multiclass classification tasks. The study compared ViT with other deep learning techniques, including Convolutional Neural Networks (CNNs) with Bi-LSTM, showcasing the potential of ViT in enhancing early clinical diagnosis and interventions in AD research. Moreover, machine learning algorithms have been utilized to improve MMSE-based screening for Alzheimer's disease by identifying predictive biomarkers [4]. Analysis of ADNI data revealed brain volume, MMSE score, and age as significant factors for enhancing accuracy and detection rates. Classification results were robust, with high AUC values distinguishing AD from normal controls and other conditions. This approach holds promise for more effective and reliable screening methods in clinical settings, potentially leading to earlier interventions and improved patient outcomes. Additionally, a CNN-based algorithm focused on MRI coronal slices of the medial temporal lobe has shown promise in distinguishing between AD patients and normal controls [9]. Validation across diverse populations affirmed its efficiency and accuracy, independent of subjects' ethnicities or demographics. By focusing on the widely used Medial Temporal Atrophy (MTA) scale, the algorithm aligned with established clinical practices and research guidelines, ensuring accurate classification while avoiding confusion with other diseases sharing similar atrophy patterns[10][11].

Chapter 3

Materials and Methods

3.1 Dependencies Installation

For the thesis research, a server provided by the Neuro-e-Care Lab at IIIT D was utilized, running Ubuntu version 22.04.1 LTS with 32 GB and 16 GB GPU. This environment supported two versions of Python: 3.7.8 and 3.10. Key tools employed included Jupyter Notebook for interactive computing, Miniconda for managing Python environments and packages, and a range of Python libraries for data analysis and machine learning.

The Python libraries utilized encompassed:

1. **NumPy:** A fundamental package for scientific computing in Python, enabling support for large, multi-dimensional arrays and matrices, alongside a suite of mathematical functions for array manipulation.
2. **Pandas:** A versatile data analysis and manipulation library, offering data structures and operations for handling tabular and time series data effectively.
3. **SciPy:** A comprehensive library for scientific and technical computing, extending the capabilities of NumPy with modules for optimization, integration, interpolation, linear algebra, and more.
4. **Scikit-learn:** A machine learning library providing tools for data mining and analysis, featuring algorithms for classification, regression, clustering, dimensionality reduction, and model selection.
5. **Matplotlib:** A plotting library facilitating the creation of static, interactive, and animated visualizations in Python, widely utilized for generating high-quality Figures.
6. **TensorFlow:** An open-source machine learning framework developed by Google, used for building and training deep learning models.
7. **PyTorch:** Another prominent open-source machine learning framework, developed by Facebook's AI Research lab (FAIR), known for its dynamic computation graph and user-friendly interface.
8. **ANTsPyNet:** A Python interface to Advanced Normalization Tools (ANTs), a software suite for processing and analyzing medical images.
9. **SimpleITK:** A simplified interface to the Insight Segmentation and Registration Toolkit (ITK), a library for segmenting and registering medical images.
10. **NiBabel:** A library for reading and writing neuroimaging data in various formats.
11. **Helpers:** A custom module or set of utility functions developed to aid specific tasks within the research.

Below are the pip commands used to install the necessary dependencies:

- pip install numpy
- pip install pandas
- pip install scipy
- pip install scikit-learn
- pip install matplotlib
- python3 -m pip install tensorflow[and-cuda]
- pip3 install torch torchvision torchaudio --index-url https://download.pytorch.org/whl/cu118torch torchvision
- pip install antspynet
- pip install SimpleITK
- pip install nibabel
- pip install helpers

3.2 Data Collection

The data utilized for this study was obtained from the Alzheimer's Disease Neuroimaging Initiative (ADNI), a longitudinal multicentre research project dedicated to developing biomarkers for the early detection and monitoring of Alzheimer's disease (AD). ADNI integrates clinical, imaging, genetic, and biochemical analyses to advance our understanding of AD pathology. Established over a decade ago, this initiative has facilitated global data sharing among researchers, fostering collaboration and accelerating progress in AD research. The comprehensive dataset provided by ADNI enables thorough investigations into the pathophysiology and progression of Alzheimer's disease, contributing significantly to the advancement of diagnostic and therapeutic approaches[12][13].
Specifically, for this study, MRI data from the ADNI dataset were utilized. The MRI data were segmented into six different classes, as represented by the file 'ADSP-PHC__ADNI_T1_1.0_10_30_2023.csv'.

3.3 Data Sorting: Organization into Class Categories

During the research, we meticulously organized the data obtained from the Alzheimer's Disease Neuroimaging Initiative (ADNI) repository into distinct categories based on two primary metadata attributes: Subject and Group. The Group attribute represents the stage of Alzheimer's Disease, and the data was classified into six distinct classes, namely Alzheimer's Disease (AD), Cognitive Normal (CN), Early Mild Cognitive Impairment (EMCI), Late Mild Cognitive Impairment (LMCI), and Mild Cognitive Impairment (MCI), Subjective Memory Complaints (SMC). This classification process was essential for the systematic analysis of the dataset, which enabled us to gain a comprehensive understanding of the diverse stages and conditions associated with Alzheimer's Disease progression. This facilitated nuanced insights and informed conclusions within the scope of this thesis work.

```python
import os
import shutil
import pandas as pd

# Path to the main folder containing subfolders with .nii files
main_folder = '/raid/home/seraj22200/adni_data/ADNI'

# Path to the CSV file containing ID and Group information
csv_file = '/raid/home/seraj22200/adni_group_separated/ADSP-PHC__ADNI_T1_1.0_10_30_2023.csv'

# Destination folder
destination_folder = '/raid/home/seraj22200/adni_group_separated/ADSP-PHC'

# Read the CSV file into a DataFrame
df = pd.read_csv(csv_file)

# Iterate through each row in the DataFrame
for index, row in df.iterrows():
    # Extract ID and Group information from the DataFrame
    file_id = str(row['Subject'])
    group = str(row['Group'])

    # Search for .nii files in the specified folder and its subfolders
    for root, dirs, files in os.walk(main_folder):
        for file in files:
            # Check if the file is a .nii file and its name contains the file_id
            if file.endswith('.nii') and file_id in file:
                # Create a destination folder based on the group
                dest_folder = os.path.join(destination_folder, group)
                os.makedirs(dest_folder, exist_ok=True)

                # Build the source and destination paths
                source_path = os.path.join(root, file)
                dest_path = os.path.join(dest_folder, file)

                # Move the file to the destination folder
                shutil.move(source_path, dest_path)
                print(f'Moved {file} to {dest_folder}')
```

```
1]
..  Moved ADNI_941_S_6052_MR_MT1__N3m_Br_20170804183926749_S585807_I882756.nii to /raid/home/seraj22200/adni_group_separated/ADSP-PHC/MCI
    Moved ADNI_941_S_6017_MR_MT1__N3m_Br_20170804175840154_S565427_I882726.nii to /raid/home/seraj22200/adni_group_separated/ADSP-PHC/MCI
    Moved ADNI_941_S_5193_MR_MT1__GradWarp__N3m_Br_20130607141715257_S190912_I375628.nii to /raid/home/seraj22200/adni_group_separated/ADSP-PHC/SMC
    Moved ADNI_941_S_5193_MR_MT1__GradWarp__N3m_Br_20130829113740072_S198235_I388033.nii to /raid/home/seraj22200/adni_group_separated/ADSP-PHC/SMC
    Moved ADNI_941_S_5193_MR_MT1__GradWarp__N3m_Br_20160609144159226_S412708_I729737.nii to /raid/home/seraj22200/adni_group_separated/ADSP-PHC/SMC
    Moved ADNI_941_S_5124_MR_MT1__GradWarp__N3m_Br_20140620091819784_S216616_I431781.nii to /raid/home/seraj22200/adni_group_separated/ADSP-PHC/SMC
```

Figure 3.3.1 Data sorting on the basis of their group

3.4 Deciphering Complexity: Navigating Exploratory Data Analysis

Among the 7096 MRI data files stored in NifTI (.nii) format, there exists a discernible demographic breakdown: 4047 of these files pertain to male patients, while the remaining 2969 correspond to female patients. Delving into the diagnostic profiles within this dataset unveils a compelling trend: the incidence of Alzheimer's Disease (AD) displays a noticeable uptick with advancing age, particularly prominent among older age cohorts. Similarly, the prevalence rates of individuals diagnosed with Cognitive Normal (CN), Early Mild Cognitive Impairment (EMCI), Late Mild Cognitive Impairment (LMCI), Mild Cognitive Impairment (MCI) and Subjective Memory Complaints (SMC)exhibit variability across different age strata, reflecting the dynamic interplay between age and cognitive health. A notable observation is the conspicuous absence of individuals aged 100-109 and those falling below the age of 50 across all diagnostic categories.

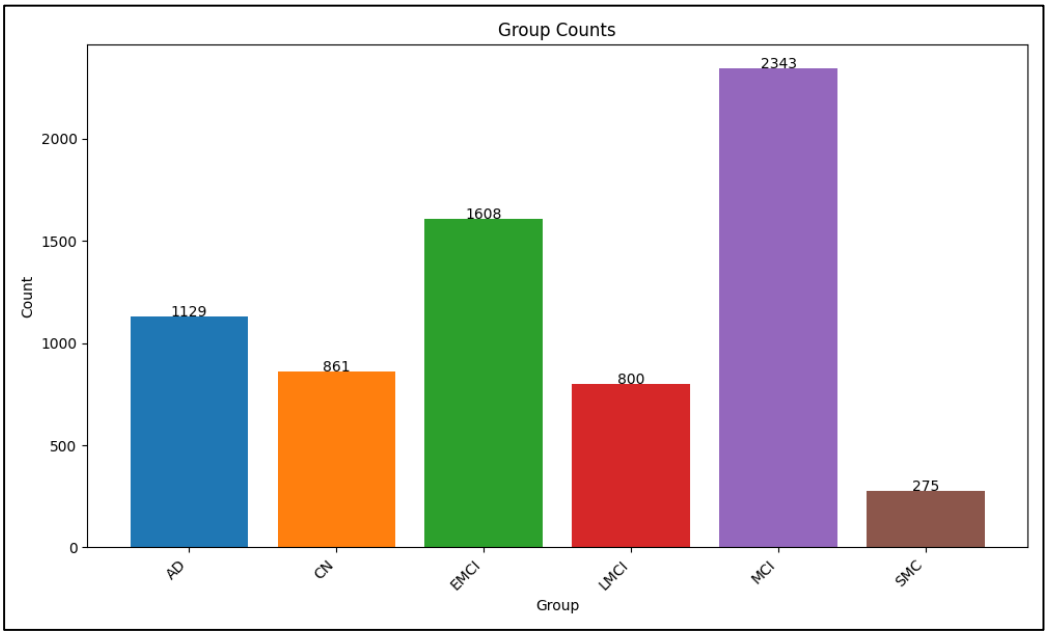

Figure:3.4.1 Histogram shows the counts of different classes

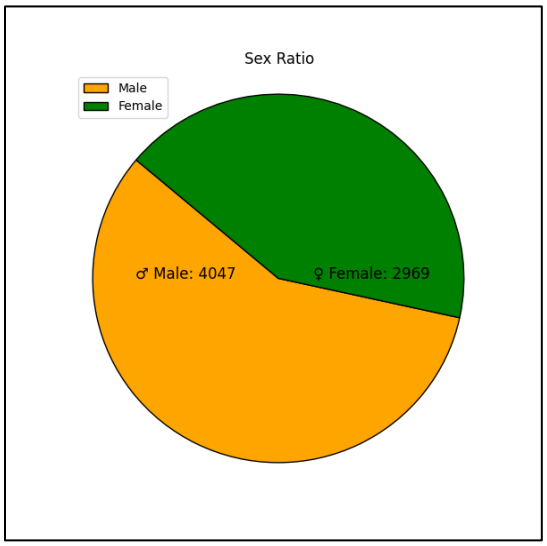

Figure:3.4.2 Pie-chart shows count of male and female MRI data

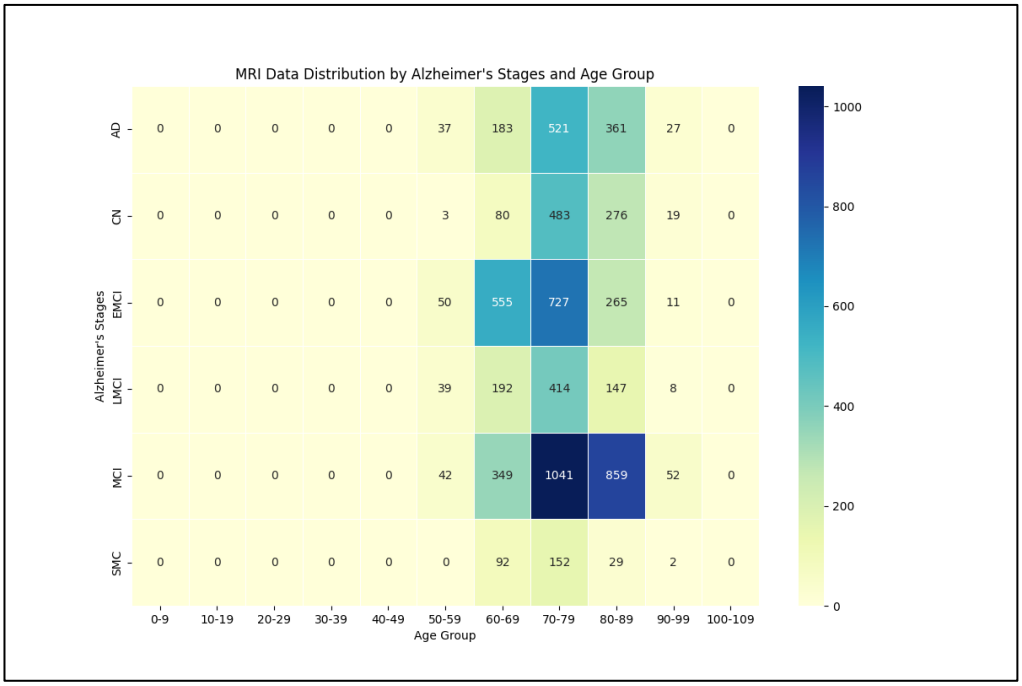

Figure:3.4.3 Heatmap show counts Alzheimer disease stage in various age groups

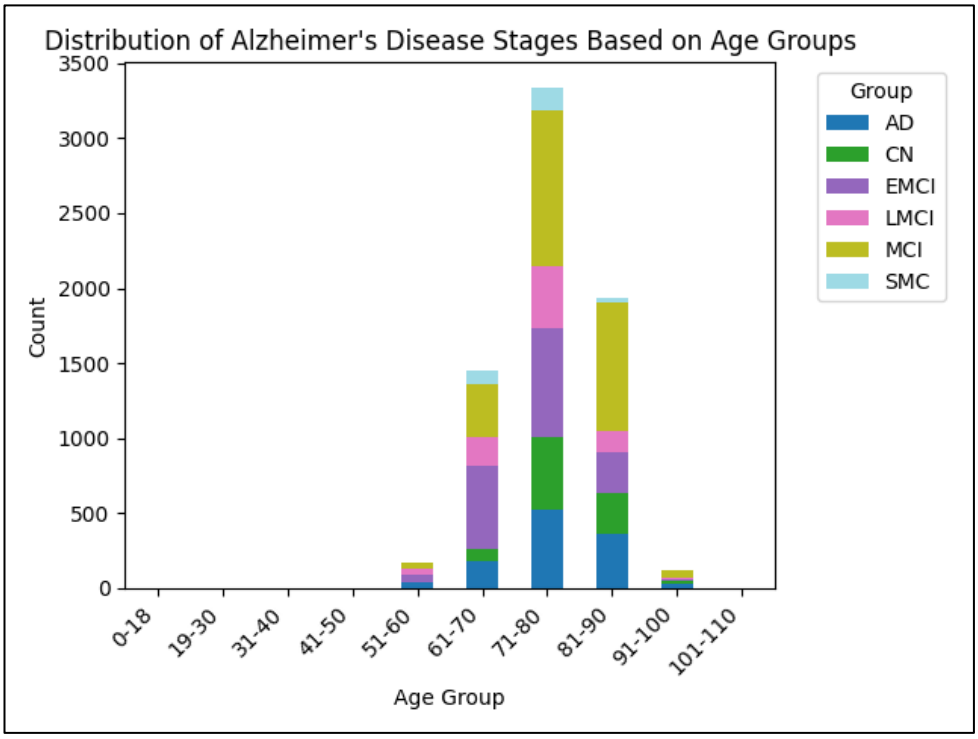

Figure:3.4.4 Bar graph show counts Alzheimer disease stage in various

3.5 Work-Flow

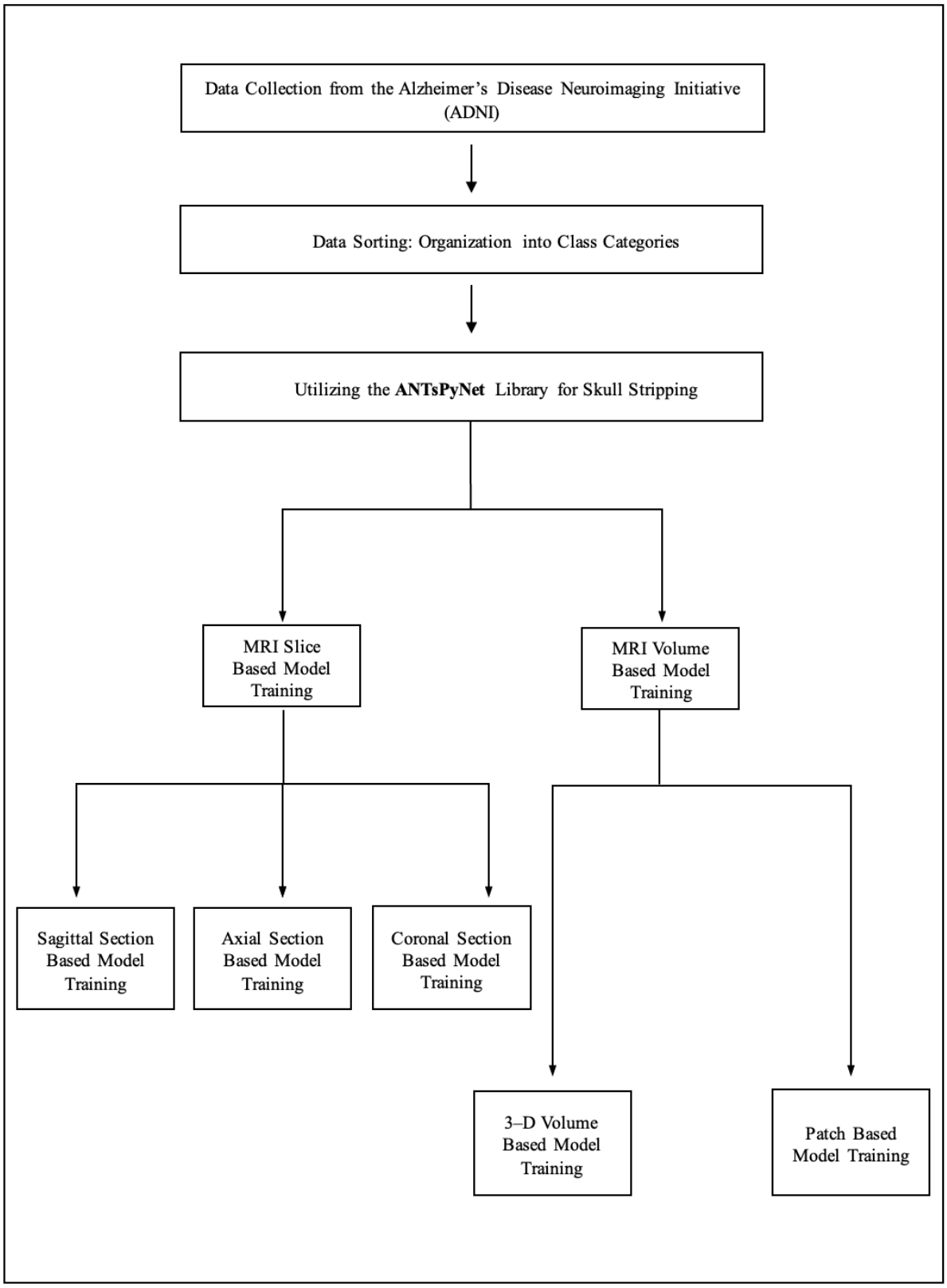

Figure:3.5.1 A structured workflow from data collection to model training

3.6 Skull Stripping with ANTsPyNet Library: An Efficient Approach for Brain Image Processing

ANTsX, or the Advanced Normalizations Tools ecosystem, encompasses a collection of open-source software libraries housing highly efficient algorithms utilized globally by scientific and research communities for the analysis and processing of biological and medical imaging data. The foundational library, ANTs, is integrated with and contributes to the NIH-sponsored Insight Toolkit. Originating in 2008 with the esteemed Symmetric Normalization image registration framework, ANTs has evolved to encompass a broader range of functionalities. Recent advancements include the integration of statistical, visualization, and deep learning capabilities via interfaces with the R statistical project (ANTsR) and Python (ANTsPy). Furthermore, extensions such as ANTsRNet and ANTsPyNet, built on TensorFlow/Keras libraries, offer various network architectures and pre-trained models tailored for specific applications. Notably, these advancements include a comprehensive deep learning approach for generating cortical thickness data from structural T1-weighted brain MRI scans, enhancing computational efficiency and accuracy compared to existing ANTs workflows. This exemplifies the significance of ANTsX as a holistic framework for medical image analysis, improving both efficiency and accuracy across multiple criteria. The ANTsX software ecosystem presents a robust framework for quantitative analysis of biological and medical imaging data. While ANTs remains a cornerstone in image registration technology within ANTsX, its scope has expanded far beyond its initial focus. This expansion not only encompasses technical advancements but also facilitates broader accessibility for users to construct customized pipelines for their studies or leverage pre-built pipelines, accessible through bash, Python, or R scripting.

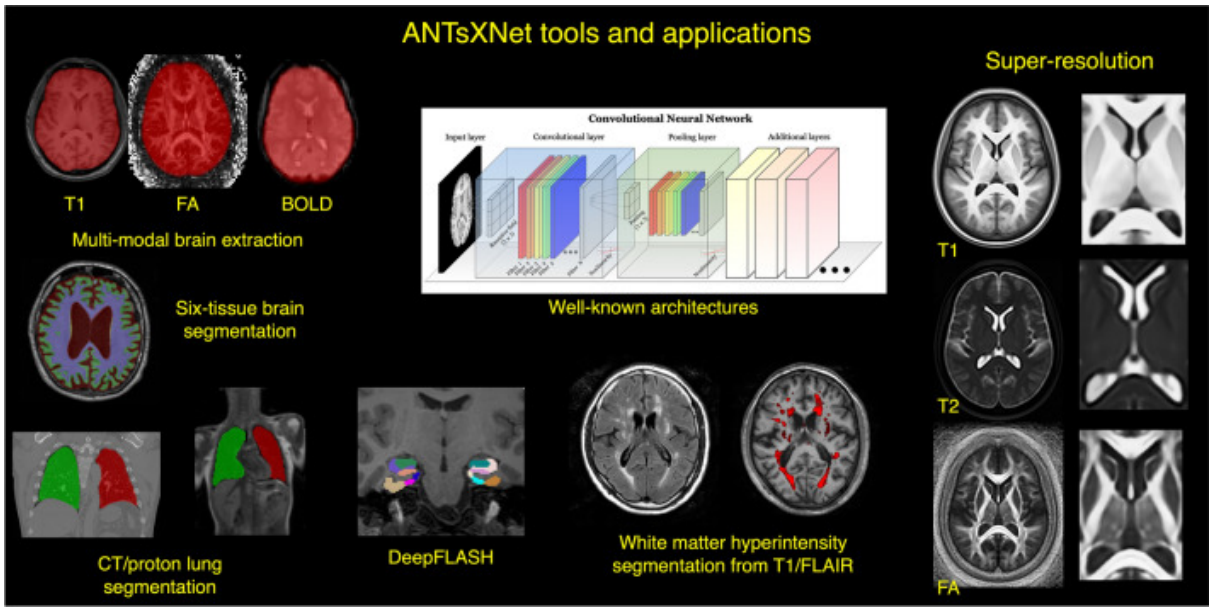

Figure:3.6.1 The ANTsRNet and ANTsPyNet deep learning toolkits exemplify the array of tools and applications accessible within the ANTs ecosystem. Leveraging the functionality of ANTs through their respective language interfaces—ANTsR (R) and ANTsPy (Python)—both libraries are constructed on the Keras/TensorFlow platform, ensuring consistency and compatibility. They employ standardized network architectures to train models and weights for various applications, including brain extraction, with the resultant models made available to the wider public[14].

3.7.1 Exploring the Critical Terminology of MRI: Orientation and Voxel Arrangement

1. **RIP (Right Inferior Posterior):** This orientation indicates a position on the right side of the body, towards the lower part (inferior), and towards the back (posterior). For example, in brain imaging, this could represent a view of the right side of the brain from the back, towards the bottom.
2. **LIP (Left Inferior Posterior):** Similar to RIP but on the left side of the body. It represents a position towards the lower part and towards the back on the left side of the body.
3. **RSP (Right Superior Posterior):** In this orientation, the position is on the right side of the body, towards the upper part (superior), and towards the back (posterior). In brain imaging, this could indicate a view of the top-right area from behind.
4. **LSP (Left Superior Posterior):** Similar to RSP but on the left side of the body. It represents a position towards the upper part and towards the back on the left side of the body.
5. **RIA (Right Inferior Anterior):** This orientation refers to a position on the right side of the body, towards the lower part (inferior), and towards the front (anterior). For example, in brain imaging, it could represent a view of the right side of the brain from the front, towards the bottom.
6. **LIA (Left Inferior Anterior):** Similar to RIA but on the left side of the body. It represents a position towards the lower part and towards the front on the left side of the body.
7. **RSA (Right Superior Anterior):** Here, the position is on the right side of the body, towards the upper part (superior), and towards the front (anterior). In brain imaging, this might show the top-right area from the front.
8. **LSA (Left Superior Anterior):** Similar to RSA but on the left side of the body. It represents a position towards the upper part and towards the front on the left side of the body.
9. **IRP (Inferior Right Posterior):** This orientation indicates a position towards the lower part (inferior) and towards the back (posterior) on the right side of the body. It might represent a view of the lower-right area from behind.
10. **ILP (Inferior Left Posterior):** Similar to IRP, but on the left side of the body. It represents a position towards the lower part and towards the back on the left side of the body.
11. **SRP (Superior Right Posterior):** This orientation refers to a position towards the upper part (superior) and towards the back (posterior) on the right side of the body. It could represent a view of the upper-right area from behind.
12. **SLP (Superior Left Posterior):** Similar to SRP, but on the left side of the body. It represents a position towards the upper part and towards the back on the left side of the body.
13. **IRA (Inferior Right Anterior):** Here, the position is towards the lower part (inferior) and towards the front (anterior) on the right side of the body. It might show the lower-right area from the front.
14. **ILA (Inferior Left Anterior):** Similar to IRA, but on the left side of the body. It represents a position towards the lower part and towards the front on the left side of the body.
15. **SRA (Superior Right Anterior):** This orientation indicates a position towards the upper part (superior) and towards the front (anterior) on the right side of the body. It might show the upper-right area from the front.

16. **SLA (Superior Left Anterior):** Similar to SRA, but on the left side of the body. It represents a position towards the upper part and towards the front on the left side of the body.
17. **RPI (Right Posterior Inferior):** This orientation refers to a position on the right side of the body, towards the back (posterior), and towards the lower part (inferior). It could represent a view of the lower-right area from below.
18. **LPI (Left Posterior Inferior):** Similar to RPI, but on the left side of the body. It represents a position towards the back and towards the lower part on the left side of the body.
19. **RAI (Right Anterior Inferior):** In this orientation, the position is on the right side of the body, towards the front (anterior), and towards the lower part (inferior). It might show the lower-right area from above.
20. **LAI (Left Anterior Inferior):** Similar to RAI, but on the left side of the body. It represents a position towards the front and towards the lower part on the left side of the body.
21. **RPS (Right Posterior Superior):** This orientation indicates a position on the right side of the body, towards the back (posterior), and towards the upper part (superior). It could represent a view of the upper-right area from below.
22. **LPS (Left Posterior Superior):** Similar to RPS, but on the left side of the body. It represents a position towards the back and towards the upper part on the left side of the body.
23. **RAS (Right Anterior Superior):** Here, the position is on the right side of the body, towards the front (anterior), and towards the upper part (superior). It might show the upper-right area from above.
24. **LAS (Left Anterior Superior):** Similar to RAS, but on the left side of the body. It represents a position towards the front and towards the upper part on the left side of the body.
25. **PRI (Posterior Right Inferior):** This orientation indicates a position towards the back (posterior) on the right side of the body, and towards the lower part (inferior). It might represent a view of the lower-right area from a different angle.
26. **PLI (Posterior Left Inferior):** Similar to PRI, but on the left side of the body. It represents a position towards the back and towards the lower part on the left side of the body.
27. **ARI (Anterior Right Inferior):** Here, the position is towards the front (anterior) on the right side of the body, and towards the lower part (inferior). It might show the lower-right area from a frontal perspective.
28. **ALI (Anterior Left Inferior):** Similar to ARI, but on the left side of the body. It represents a position towards the front and towards the lower part on the left side of the body.
29. **PRS (Posterior Right Superior):** This orientation indicates a position towards the back (posterior) on the right side of the body, and towards the upper part (superior). It could represent a view of the upper-right area from a different angle.
30. **PLS (Posterior Left Superior):** Similar to PRS, but on the left side of the body. It represents a position towards the back and towards the upper part on the left side of the body.
31. **ARS (Anterior Right Superior):** Here, the position is towards the front (anterior) on the right side of the body, and towards the upper part (superior). It might show the upper-right area from a frontal perspective.
32. **ALS (Anterior Left Superior):** Similar to ARS, but on the left side of the body. It represents a position towards the front and towards the upper part on the left side of the body.

33. **SPR (Superior Posterior Right):** Similar to IPR, but towards the upper part (superior) on the right side of the body. It represents a position towards the back and towards the upper part on the right side.
34. **IAR (Inferior Anterior Right):** This orientation indicates a position towards the lower part (inferior) and towards the front (anterior) on the right side of the body. It might show the front-right area from below.
35. **SAR (Superior Anterior Right):** Similar to IAR, but towards the upper part (superior) on the right side of the body. It represents a position towards the front and towards the upper part on the right side.
36. **IPL (Inferior Posterior Left):** This orientation indicates a position towards the lower part (inferior) and towards the back (posterior) on the left side of the body. It could represent a view of the back-left area from below.
37. **SPL (Superior Posterior Left):** Similar to IPL, but towards the upper part (superior) on the left side of the body. It represents a position towards the back and towards the upper part on the left side.
38. **IAL (Inferior Anterior Left):** This orientation indicates a position towards the lower part (inferior) and towards the front (anterior) on the left side of the body. It might show the front-left area from below.
39. **SAL (Superior Anterior Left):** Similar to IAL, but towards the upper part (superior) on the left side of the body. It represents a position towards the front and towards the upper part on the left side.
40. **PIR (Posterior Inferior Right):** This orientation indicates a position towards the back (posterior) and towards the lower part (inferior) on the right side of the body. It might represent a view of the lower-right area from a different angle.
41. **PSR (Posterior Superior Right):** Similar to PIR, but towards the upper part (superior) on the right side of the body. It represents a position towards the back and towards the upper part on the right side.
42. **AIR (Anterior Inferior Right):** This orientation indicates a position towards the front (anterior) and towards the lower part (inferior) on the right side of the body. It might show the lower-right area from a frontal perspective.
43. **ASR (Anterior Superior Right):** Similar to AIR, but towards the upper part (superior) on the right side of the body. It represents a position towards the front and towards the upper part on the right side.
44. **PIL (Posterior Inferior Left):** This orientation indicates a position towards the back (posterior) and towards the lower part (inferior) on the left side of the body. It might represent a view of the lower-left area from a different angle.
45. **PSL (Posterior Superior Left):** Similar to PIL, but towards the upper part (superior) on the left side of the body. It represents a position towards the back and towards the upper part on the left side.
46. **AIL (Anterior Inferior Left):** This orientation indicates a position towards the front (anterior) and towards the lower part (inferior) on the left side of the body. It might show the lower-left area from a frontal perspective.
47. **ASL (Anterior Superior Left):** Similar to AIL, but towards the upper part (superior) on the left side of the body. It represents a position towards the front and towards the upper part on the left side.

3.7.2 ANTsPyNet Approach to Brain Extraction Procedure

The MRI dataset exhibits a volumetric structure characterized by dimensions (166, 256, 256), which respectively denote depth (Z), length (X), and width (Y). This arrangement signifies the dataset's composition of slices, along with their corresponding spatial dimensions. Upon input to the ANTsPyNet library, the dataset undergoes pre-processing procedures. Initially, a segmentation algorithm is employed to delineate the complete brain region. Subsequent to segmentation, the identified brain region is extracted, facilitating the removal of extraneous areas or artifacts. The resulting volume, now comprising solely the isolated brain structure, is then retained for subsequent stages of model training and analytical processes.

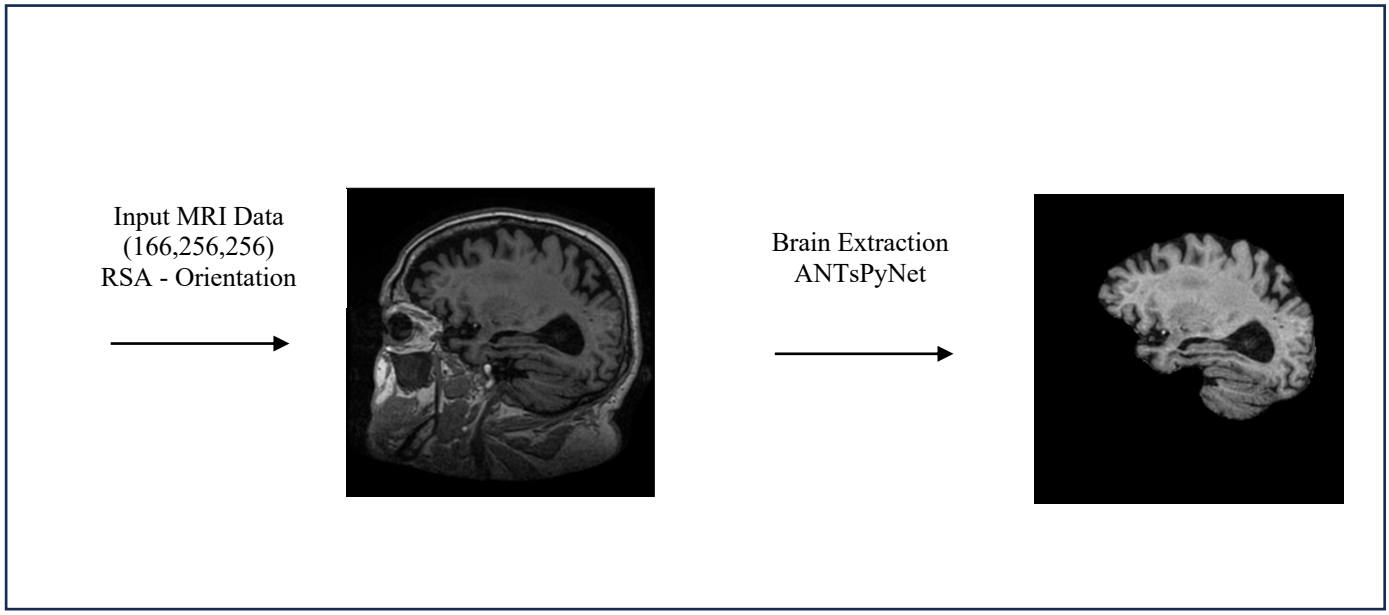

Figure:3.7.2.1 Brain extraction procedure

Chapter 4

Deep Learning-Based Framework for Disease Prediction from MRI Data: Methodology and Performance Analysis

4.1 Deep Learning Approach for Disease Detection in MRI Images: A 2D CNN – Slice Based Model Training for multiclass classification

4.1.1.1 Introduction

Detecting diseases in medical imaging, mainly through deep learning techniques like Convolutional Neural Networks (CNNs), is a burgeoning field with profound implications for diagnosis and treatment. In this context, researchers have explored innovative approaches for disease detection, often leveraging various orientations and sections of brain MRI images.

In medical imaging research, a burgeoning avenue lies in the accurate detection of neurological diseases, notably Alzheimer's disease, leveraging innovative methodologies. Particularly noteworthy is the utilization of distinct MRI orientations—RSA (Right Superior Anterior) for sagittal sections, ASL (Anterior Superior Left) for coronal sections, and SLA (Superior Left Anterior) for axial sections[14].

These orientations serve as pivotal frameworks for comprehensive brain analysis, each offering unique insights into brain anatomy and pathology. By integrating all three orientations into the research paradigm, a holistic understanding of neurological conditions is fostered, transcending the limitations of single-section analysis.

The RSA orientation, with its focus on sagittal sections, provides a standardized platform for delineating brain structures and abnormalities. Simultaneously, the ASL orientation offers a complementary perspective on coronal sections, while the SLA orientation enriches the analysis of axial sections[15].

The integration of these orientations into the training process of deep learning (DL) models, particularly Convolutional Neural Networks (CNNs), holds immense promise for accurate disease classification across diverse MRI sections. By capitalizing on the distinct features and patterns discernible in each orientation, researchers aim to develop robust models capable of detecting neurological conditions with high specificity and sensitivity.

This comprehensive approach underscores the multifaceted nature of neurological diseases and the importance of embracing diverse perspectives in diagnostic endeavours. Through the synergistic integration of MRI orientations and advanced machine learning techniques, researchers aspire to propel the field of medical imaging towards enhanced diagnostic accuracy and improved patient care.

Training a CNN-based model typically begins with the compilation of a dataset containing labelled MRI images from different orientations and sections of the brain. These images include sagittal views, offering unique insights into brain anatomy and pathology. Pre-processing techniques are applied to the dataset to improve image quality and remove noise, ensuring that the input data is suitable for model training.

The CNN architecture is then designed and implemented, comprising multiple layers of convolutional, pooling, and fully connected layers. These layers are tasked with extracting hierarchical features from the input images, enabling the model to learn discriminative representations relevant to disease detection. During training, the model iteratively adjusts its internal parameters using optimization algorithms like backpropagation and gradient descent, minimizing prediction errors and improving overall performance. Once trained, the CNN can be deployed for disease detection tasks on unseen MRI scans. The models analyze new images of their orientation or section type, identifying potential abnormalities and providing predictions regarding disease presence.

4.1.1.2 Data split Explanation for the 2D CNN slice based model.

In the original data downloaded from the ADNI source. There was total 7016 data. 80% (5615 patients) of the subjects were used for training. Remaining (1401 patient) were used for validation. There is no overlap between train and validation patient.

The data count of all six classes as follow:

For training

MCI:1875, EMCI: 1287, AD:904, CN:689, LMCI:640, SMC:220

For validation

MCI:468, EMCI: 321, AD:225, CN:172, LMCI:160, SMC:55

After the spilt of the data further we extracted the 10 slice from each subject and made another slice based data. Now the slice based data count will as follow:

For training

MCI:18750, EMCI: 12870, AD:9040, CN:6890, LMCI:6400, SMC:2200

For validation

MCI:4680, EMCI: 3210, AD:2250, CN:1720, LMCI:1600, SMC:550

All the data is unique, with no overlap between the training and validation datasets. The subsequent sections comprehensively explain the three aspects of MRI data pre-processing.

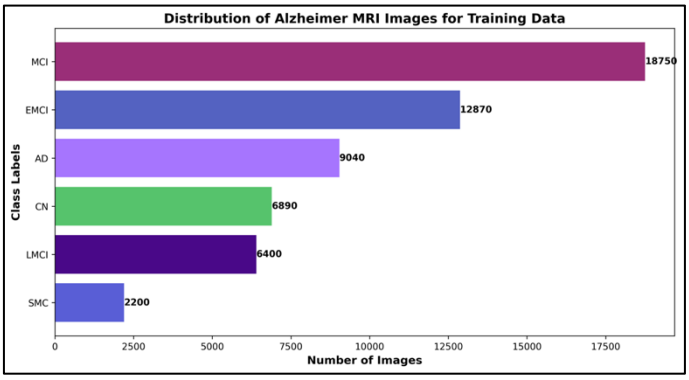

Figure: 4.1.1

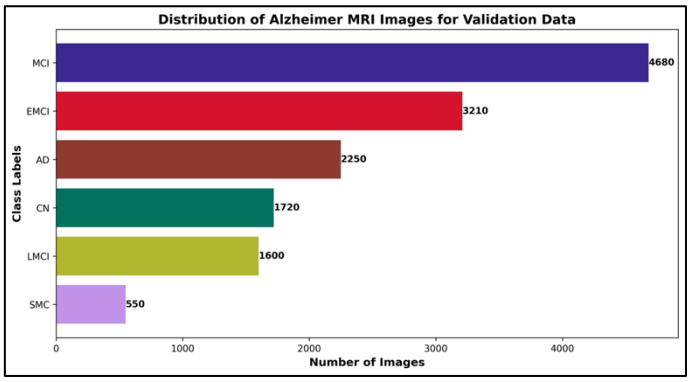

Figure: 4.1.2

Figure:4.1.1 Distribution of Alzheimer's MRI Data for Model Training with Class Assignments for 2D CNN

Figure:4.1.2 Distribution of Alzheimer's MRI Data for Model Validation with Class Assignments for 2D CNN

4.1.2 Data Pre-processing for Sagittal Section

This study utilized data sourced from ADNI, comprising various types of processed MRI images. The data underwent pre-processing using ANTsPyNet, a library facilitating brain extraction. Following brain extraction, the RSA (Right Superior Anterior) orientation for sagittal sections was employed, incorporating 10 slices from each subject in some subject 10 slices have been taken to construct the model. The selection of slice indices varied across different types of processed MRI images, guided by visualizations of brain slices included for model training and performance evaluation.

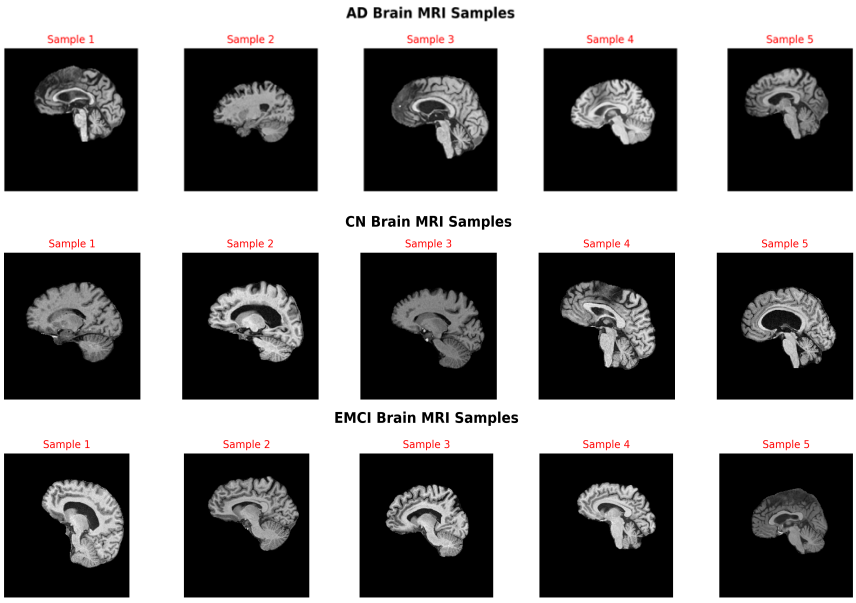

Figure:4.1.2.1 Visualization of Sagittal Section MRI samples depicting different stages of Alzheimer's Disease. From top: Sample of AD (Alzheimer's Disease), CN (Cognitive Normal), EMCI (Early Mild Cognitive Impairment).

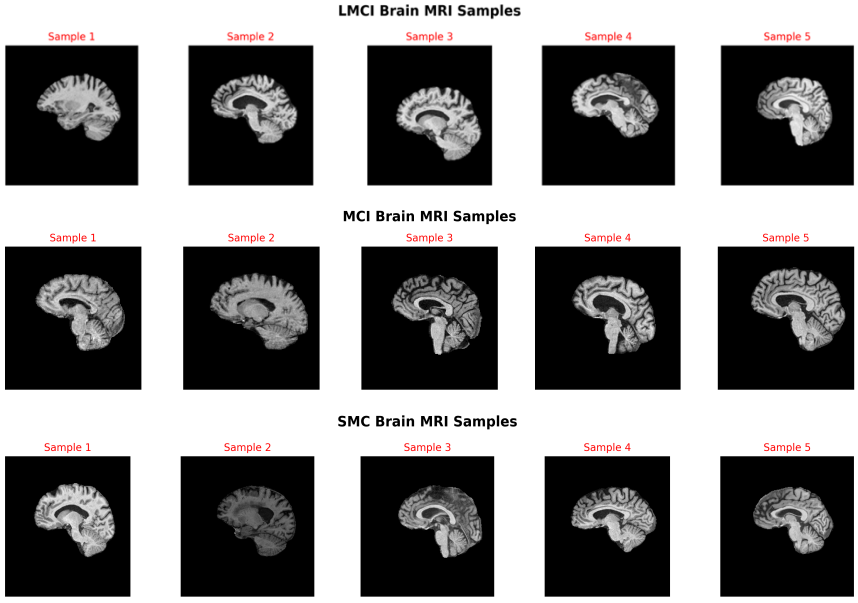

Figure:4.1.2.2 Visualization of Sagittal Section MRI samples depicting different stages of Alzheimer's Disease. From top: Sample of LMCI (Late Mild Cognitive Impairment), MCI (Mild Cognitive Impairment), SMC (Subjective Memory Complaints).

4.1.3 Data Pre-processing for Axial Section

This research employed data obtained from ADNI, encompassing diverse sets of processed MRI images. The data was prepared through pre-processing techniques utilizing ANTsPyNet, a library specialized in brain extraction. After the extraction process, the SLA (Superior Left Anterior) approach was applied to axial sections, utilizing 10 slices from each participant to build the model. The selection of slice indices was adjusted according to the specific characteristics of different types of processed MRI images, guided by visual assessments of brain slices utilized for both model training and performance assessment[16].

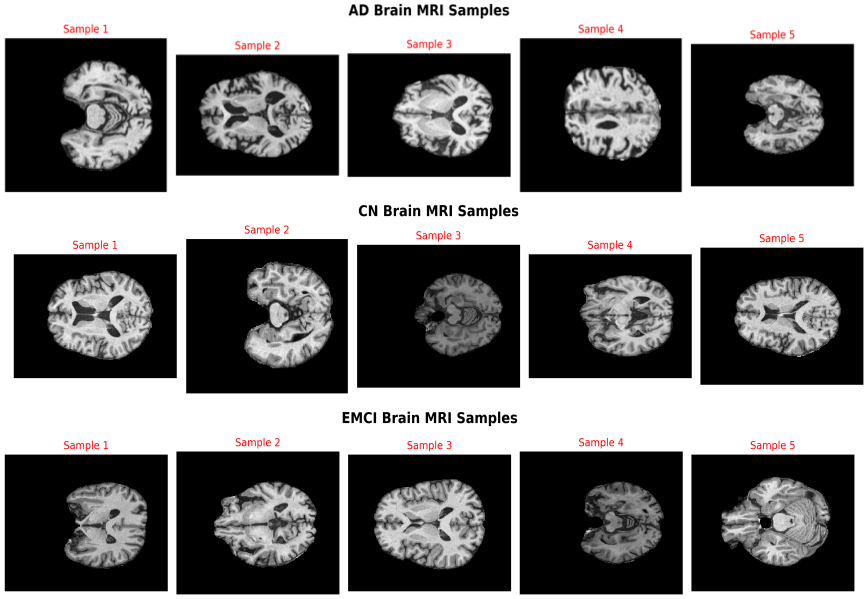

Figure:4.1.3.1 Visualization of Axial Section MRI samples depicting different stages of Alzheimer's Disease. From top: Sample of AD (Alzheimer's Disease), CN (Cognitive Normal), EMCI (Early Mild Cognitive Impairment).

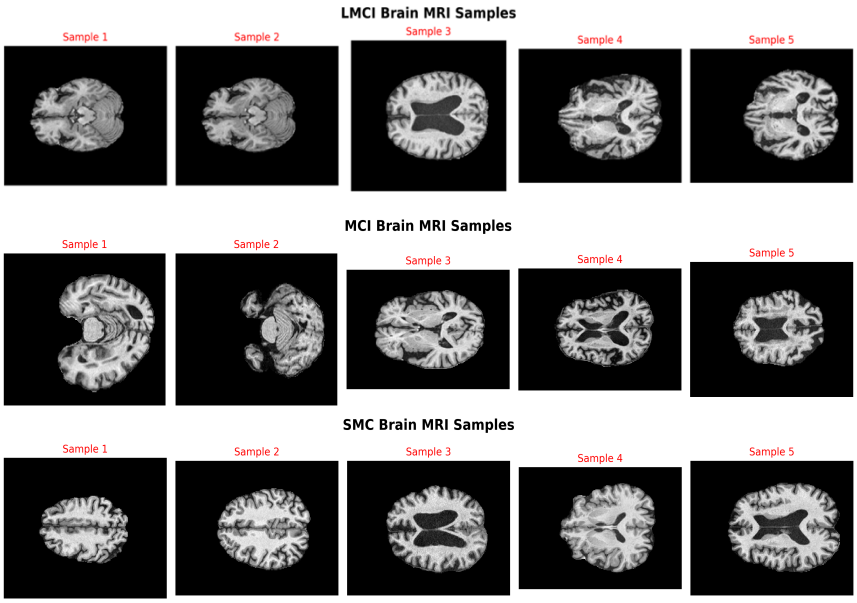

Figure:4.1.3.2 Visualization of Axial Section MRI samples depicting different stages of Alzheimer's Disease. From top: Sample of LMCI (Late Mild Cognitive Impairment), MCI (Mild Cognitive Impairment), SMC (Subjective Memory Complaints).

4.1.4 Data Pre-processing for Coronal Section

This study used diverse sets of processed MRI images from ADNI. The data underwent pre-processing using ANTsPyNet for brain extraction. Following extraction, the ASL (Anterior Superior Left) method was applied to coronal sections, using 10 slices per participant for model development. Slice indices were customized based on specific image characteristics, guided by visual assessments of brain slices used in model training and performance evaluation. This approach ensured the accuracy of the research findings while using established techniques and datasets. The methodology involved customizations to optimize model construction and evaluation, contributing to the originality and reliability of the study.

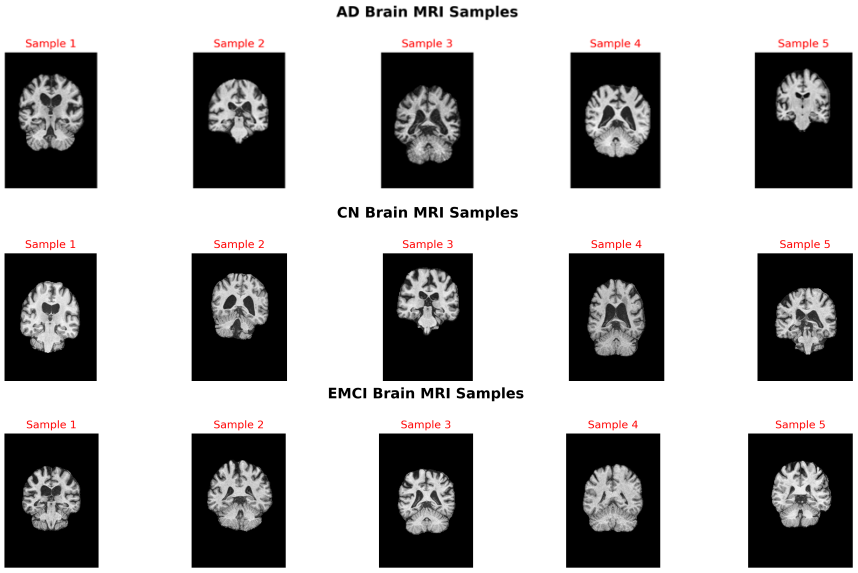

Figure:4.1.4.1 Visualization of Coronal Section MRI samples depicting different stages of Alzheimer's Disease. From top: Sample of AD (Alzheimer's Disease), CN (Cognitive Normal), EMCI (Early Mild Cognitive Impairment).

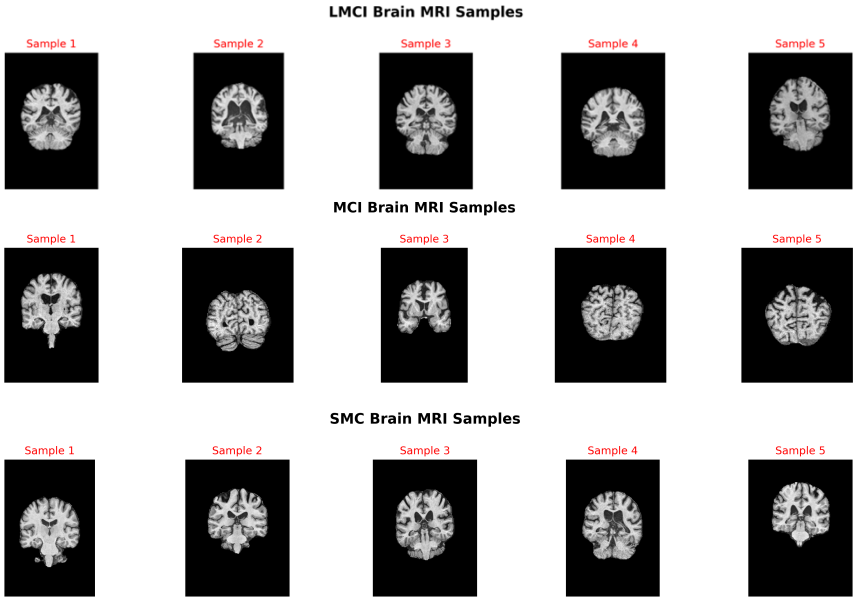

Figure:4.1.4.2 Visualization of Coronal Section MRI samples depicting different stages of Alzheimer's Disease. From top: Sample of LMCI (Late Mild Cognitive Impairment), MCI (Mild Cognitive Impairment), SMC (Subjective Memory Complaints).

4.1.5 Architecture overview for 2D slice-based classification

1. Input Layer: The model commences with a convolutional layer (Conv2D) featuring 16 filters, each sized 3x3. This layer utilizes the ReLU (Rectified Linear Unit) activation function, expressed as[17]:

   $\text{ReLU}(x)=\max(0,x)$

   The input shape is set to (128, 128, 3), indicating that it anticipates images sized 128x128 with three colour channels (RGB).

2. Max Pooling: Following each convolutional layer, there's a max-pooling layer (MaxPooling2D) employing a pool size of 2x2. Max pooling reduces the spatial dimensions of the representation, aiding in diminishing computational complexity and curbing overfitting.

3. Convolutional Layers: Two additional convolutional layers ensue, each featuring an increasing number of filters (32 and 128 respectively), employing the same configuration as the initial layer.

4. Flattening: Post the final convolutional layer, the output is flattened into a vector using the Flatten layer. This prepares the data for input into the fully connected layers.

5. Fully Connected Layers: The architecture incorporates three fully connected (Dense) layers, housing 128, 64, and 6 neurons respectively. The ReLU activation function is employed for the first two layers, defined as:

   $\text{ReLU}(x)=\max(0,x)$

   For the last layer, the softmax activation function is used. The softmax function converts the network's raw output into probability scores for each class, enabling multi-class classification. It's expressed as:

   $$\text{softmax}(x_i) = \frac{e^{x_i}}{\sum_{j=1}^{N} e^{x_j}}$$

   Where:
   • x_i is the raw score for class i.
   • N is the total number of classes.

6. Kernel Initialization (He Normal): Kernel initialization is a crucial step in training neural networks, particularly convolutional neural networks (CNNs). It involves initializing the weights of the kernels (filters) in the convolutional layers[18].

   The He Normal initialization technique is employed in this architecture. It initializes the weights of the kernels using a Gaussian distribution with a mean of 0 and a standard deviation calculated based on the number of input and output units. Specifically, the standard deviation is calculated as where $\sqrt{\frac{2}{nin}}$ n_{in} is the number of input units.
   This initialization scheme is particularly well-suited for ReLU activation functions, ensuring efficient learning by effectively propagating gradients during training.

7. Compilation: The model is compiled utilizing the Adam optimizer and sparse categorical cross-entropy loss function, suitable for multi-class classification tasks with integer labels.

This architecture is well-structured for image classification tasks, particularly when dealing with relatively small images (128x128) and a moderate number of classes (6 in this case). It leverages standard components like convolutional and pooling layers alongside fully connected layers and incorporates popular techniques such as ReLU activation, softmax function, and He Normal weight initialization for enhanced training performance.

4.1.5.1 Model Architecture Strategies for Sagittal Section of 2D CNN

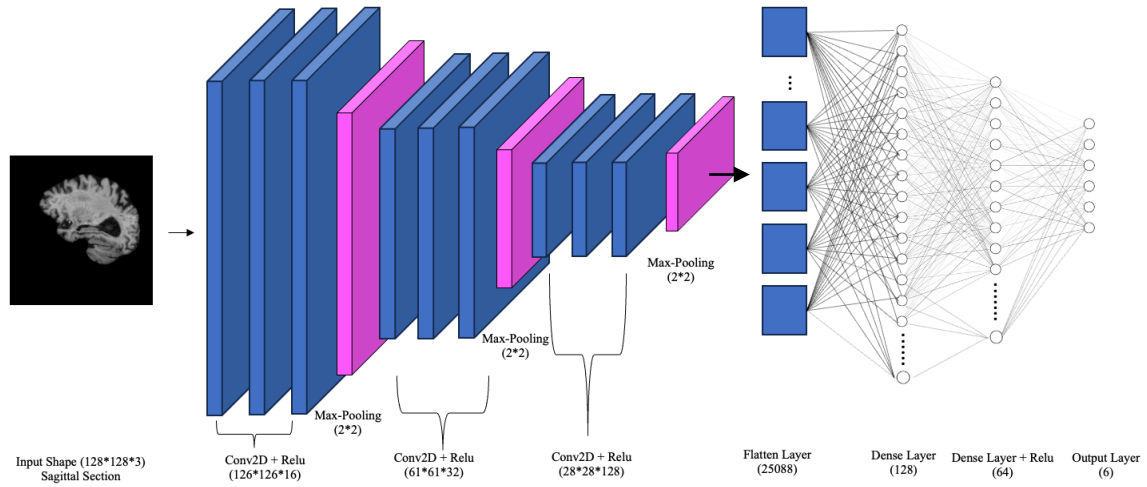

Figure:4.1.5.1.1 CNN based model architecture for sagittal section of the brain.

4.1.5.2 Model Architecture Strategies for Axial Section of 2D CNN

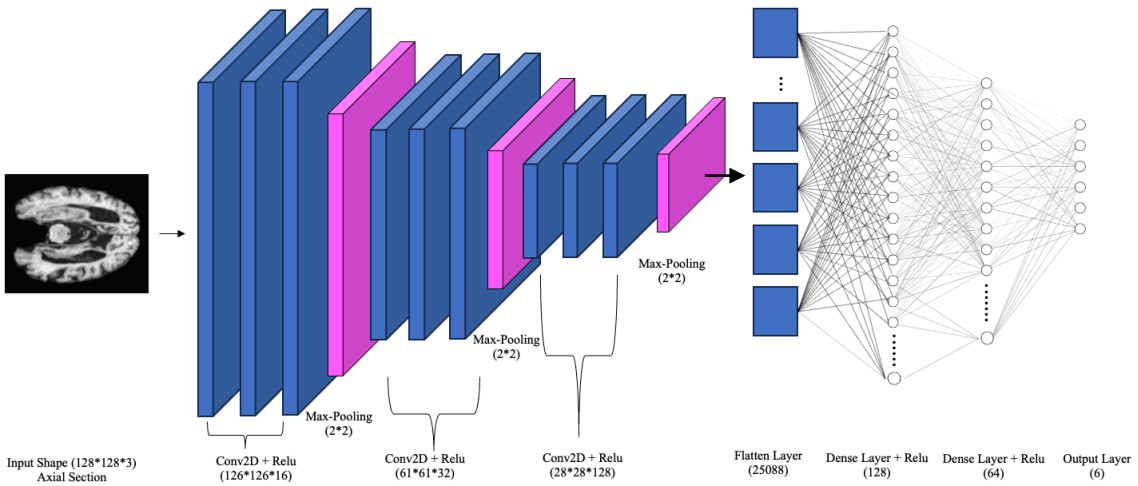

Figure:4.1.5.2.1 CNN based model architecture for axial section of the brain

4.1.5.3 Model Architecture Strategies for Coronal Section of 2D CNN

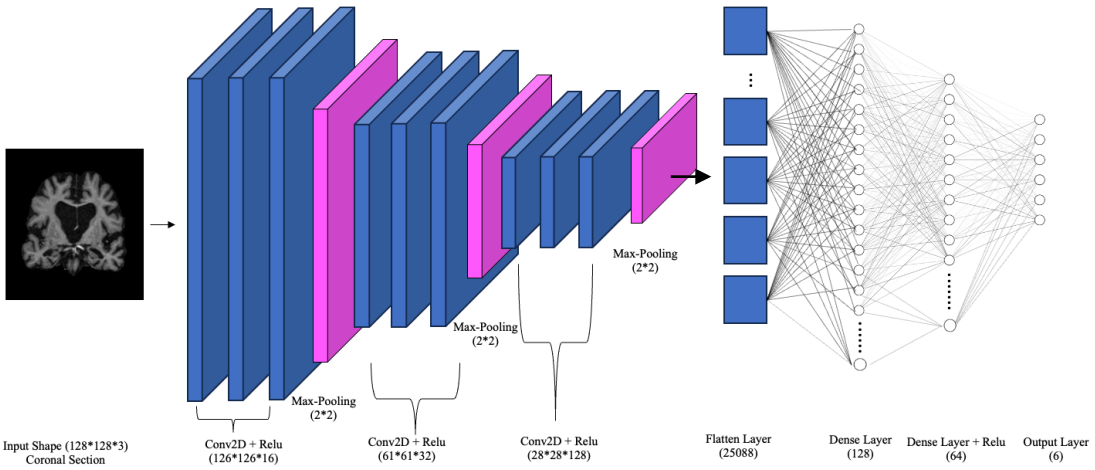

Figure:4.1.5.3.1 CNN based model architecture for coronal section of the brain.

4.2 Empowering Alzheimer's Disease Classification in MRI via 3D CNN-based Models

4.2.1 Overview

A 3D CNN, or Convolutional Neural Network, is a type of deep learning model used for processing volumetric data, such as medical images or video. Unlike traditional CNNs, which work with 2D data like images, 3D CNNs operate on three-dimensional data, allowing them to capture spatial and temporal information across width, height, and depth.
In the context of ADNI data analysis, a 3D CNN could be employed to analyze brain scans from the Alzheimer's Disease Neuroimaging Initiative (ADNI). Each input to the network would be a 3D volume representing the brain structure of a patient. The 3D CNN would learn to extract relevant features from these volumes and classify them into different categories, such as healthy or Alzheimer's affected.

In the scenario presented, the ADNI dataset comprises 7016 data volumes, with each volume has either of six classes Alzheimer's Disease. There was total 7016 data. 80% (5615 patients) of the subjects were used for training. Remaining (1401 patient) were used for validation. There is no overlap between train and validation patient.
During training, the 3D CNN iteratively processes the training data, adjusting its parameters (weights) based on the error between predicted and actual labels. This process, known as backpropagation, aims to optimize the model's performance on the training data. The validation dataset is then used to evaluate the model's performance on unseen data, providing insights into its generalization capabilities.

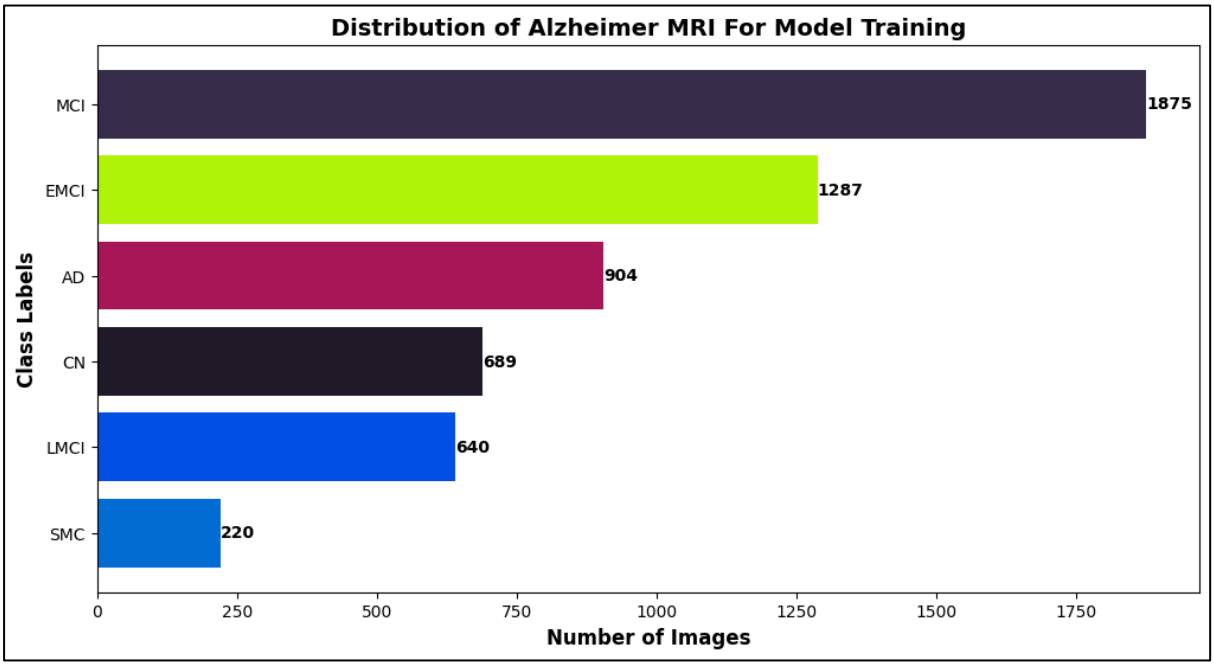

Figure:4.2.1.1 Distribution of Alzheimer's MRI Data for Model Training with Class Assignments

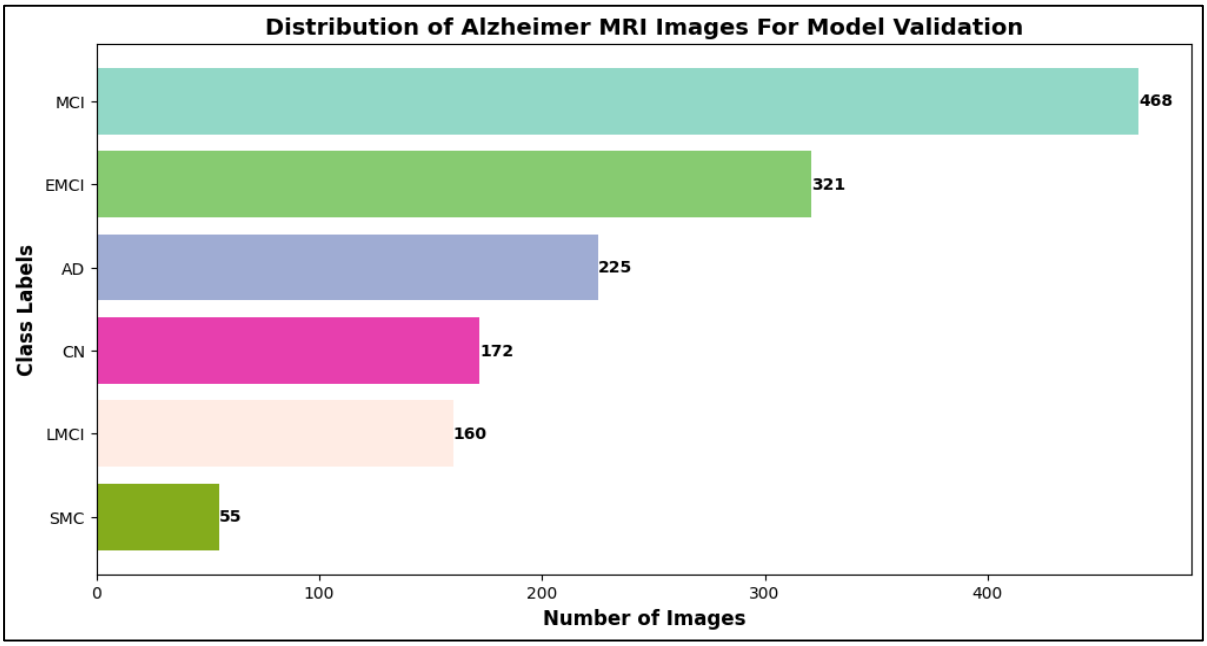

Figure:4.2.1.2 Distribution of Alzheimer's MRI Data for Model Validation with Class Assignments

4.2.2 Preparation of Data for Training the 3D CNN Model

Within the dataset, variations exist in the height, width, and number of slices among different patients. To standardize this variability following skull stripping, the depth was adjusted to 166 during model processing. This adjustment accommodated variations such as data sets containing 256, 192, or 166 slices. Subsequently, to ensure uniformity in pixel values, the data underwent normalization using min-max scaling.

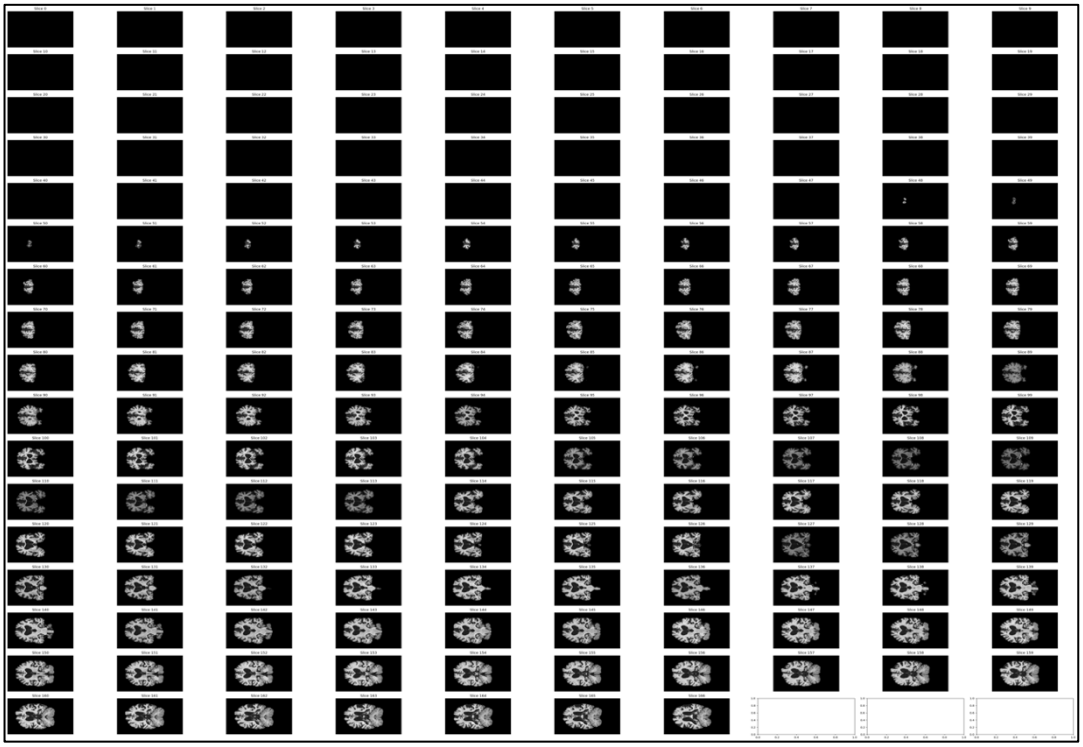

Figure:4.2.2.1 Visualization of MRI data used for the 3D CNN

4.2.3 Architecture Overview

The 3D Convolutional Neural Network (CNN) is designed to process medical image data with dimensions of 128x128x166. Each patient file undergoes resizing before being fed into the model for training. The input layer is configured to accept volumes of data with dimensions 128x128x166 and a single grayscale channel. The network consists of three convolutional layers, each followed by ReLU activation and L2 regularization. The first layer has 16 filters with a kernel size of 3x3x3, the second layer has 32 filters, and the third layer has 64 filters. Max pooling layers are applied after each convolutional layer to reduce spatial dimensions by a factor of 2 along each dimension using a pool size of 2x2x2. Batch normalization layers are applied after max-pooling to normalize activations and stabilize training. The output from the last convolutional layer is flattened into a 1D vector before being fed into fully connected layers. Two dense layers follow: the first with 128 neurons and ReLU activation, and the second with 64 neurons and ReLU activation. A dropout layer with a dropout rate of 0.1 is included to prevent overfitting. The output layer consists of 6 neurons for classification tasks, utilizing softmax activation to output class probabilities. This architecture is optimized for efficiently processing volumetric medical image data for classification purposes.

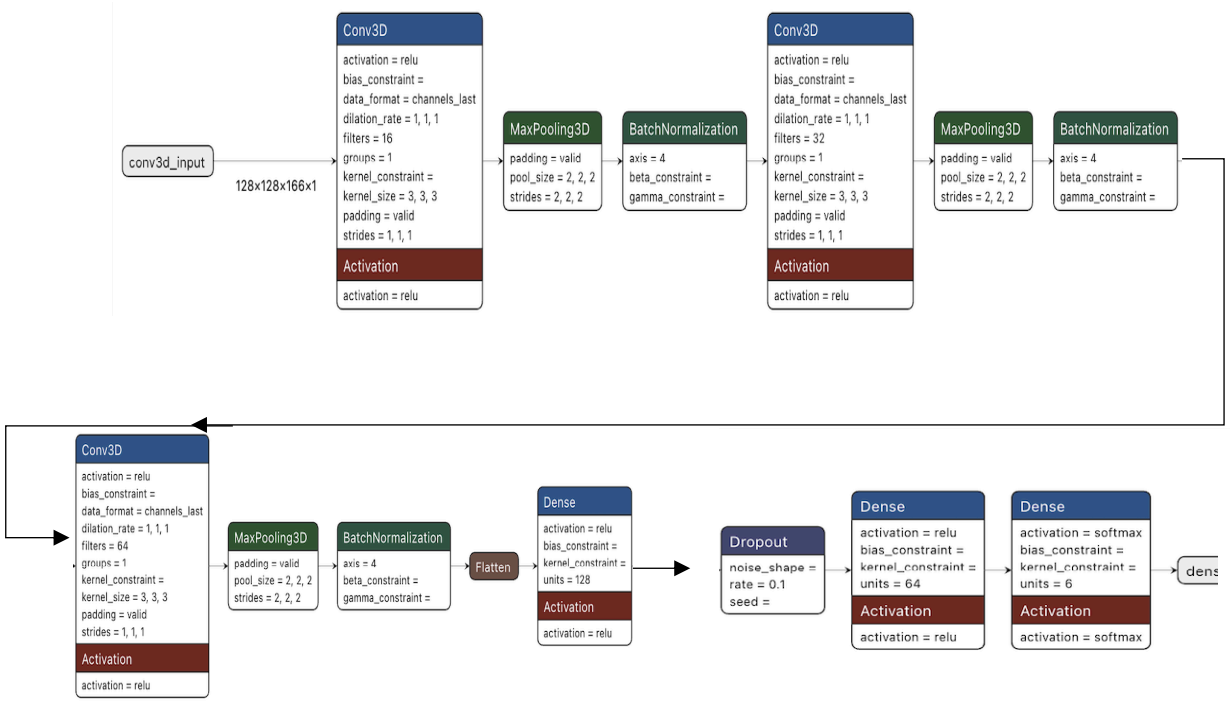

Figure: 4.2.3.1 Implementation of a 3D-CNN model for the purpose of multiclass classification

4.3 Alzheimer's Disease Detection via Patch-Based Convolutional Neural Networks

4.3.1.1 Overview

Detecting Alzheimer's Disease using Patch-Based Convolutional Neural Networks (CNNs) involves the application of CNNs to identify and classify Alzheimer's disease based on MRI data analyzed at the patch level. Alzheimer's disease is a progressive neurodegenerative disorder marked by memory loss, cognitive impairment, and other neurological symptoms. Early and accurate detection of Alzheimer's is essential for timely intervention and treatment. In this approach, MRI brain images are divided into smaller patches, each representing a specific region of the brain. By segmenting the images into these patches, the CNN can focus on local features and patterns that may provide critical information relevant to Alzheimer's disease. The ResNet-18 architecture is employed, which consists of multiple convolutional, pooling, and fully connected layers. These layers extract hierarchical features from the input patches, identifying spatial patterns indicative of Alzheimer's. The network is trained on a dataset of labeled MRI brain images, with each image annotated according to its disease status. During training, the CNN learns to differentiate between patches from brains affected by Alzheimer's and those from healthy brains. The model's parameters are optimized through backpropagation and other algorithms to reduce classification errors. The dataset used is sourced from the Alzheimer's Disease Neuroimaging Initiative (ADNI) and includes 7016 MRI volumes categorized into six groups related to Alzheimer's Disease. There was total 7016 data. 80% (5615 patients) of the subjects were used for training. Remaining (1401 patient) were used for validation. There is no overlap between train and validation patient.

The distribution of data across the six classes is as follows:

For training: 1875 of MCI, 1287 of EMCI, 904 of AD, 689 of CN, 640 of LMCI, and 220 of SMC.

For validation: 468 of MCI, 321 of EMCI, 225 of AD, 172 of CN, 160 of LMCI, and 55 of SMC.

4.3.2 Data Pre-processing for the patch-based CNN

The process of preparing the data for model training began with obtaining the necessary datasets from ADNI (Alzheimer's Disease Neuroimaging Initiative) sources. Since MRI scans typically capture more than just the brain, such as surrounding tissues like the skull and mouth, a brain extraction step was essential. This extraction process removes non-brain regions from the images, reducing unnecessary noise that could interfere with the model's ability to learn meaningful patterns related to Alzheimer's disease.

To perform brain extraction, sophisticated algorithms and tools like the ANTsPyNet Library were employed. These tools are specifically designed to accurately identify and isolate the brain within MRI scans, ensuring that only relevant brain data is retained for further analysis.

After brain extraction, the data went through a brain correction phase using the ANTsPyNet Library. This step helps in correcting any potential distortions or inconsistencies in the brain images, ensuring that the data is as accurate and reliable as possible before being used for training.

Finally, the preprocessed data was scaled. Scaling involves adjusting the range of values in the data to a standard scale, typically between 0 and 1 or -1 and 1. This step is crucial for ensuring that the model's training process is more stable and efficient, as it helps prevent certain features from dominating the learning process and ensures that all features contribute equally to the model's training.

By following this detailed data preparation pipeline, the training data was optimized to provide the best possible input for the convolutional neural network (CNN) model, enhancing its ability to accurately detect and classify Alzheimer's disease from MRI scans.

4.3.3 Model Architecture

1. **Model Architecture**: The architecture used for training the model is similar to ResNet-18. ResNet-18 is a convolutional neural network (CNN) architecture commonly used for image classification tasks. It consists of several convolutional layers with residual connections, allowing for the training of very deep networks[19].
2. **Input Shape**: The input shape of the model is specified as (100, 1, 128, 128), where:
    a. 100: Represents the number of slices.
    b. 1: Indicates the number of channels. In this case, it's a grayscale image with a single channel.
    c. 128x128: Denotes the width and height of each input slice.
3. **Batch Processing**: During model training, data is fed to the model in batches. The size of each batch is denoted as 'n'. The model processes 'n' batches of patient data at a time. This batch processing allows for more efficient training by leveraging parallelism and reducing memory requirements.
4. **Voting Mechanism**: After all the features are selected and processed, the model performs a voting mechanism for prediction. This means that instead of making predictions based on individual data points, the model aggregates predictions from multiple instances within a batch. This helps in producing more accurate results by considering the collective input.
5. **Prediction Concept**: The concept of mode is used for prediction. Mode refers to the value that appears most frequently in a set of data. In this context, the model identifies the class prediction that occurs most frequently across all the predictions within a batch. If one class occurs more frequently than others (i.e., if it is the mode), the model considers it as the final prediction. This approach aims to increase the robustness of predictions by considering the most common prediction across multiple instances.

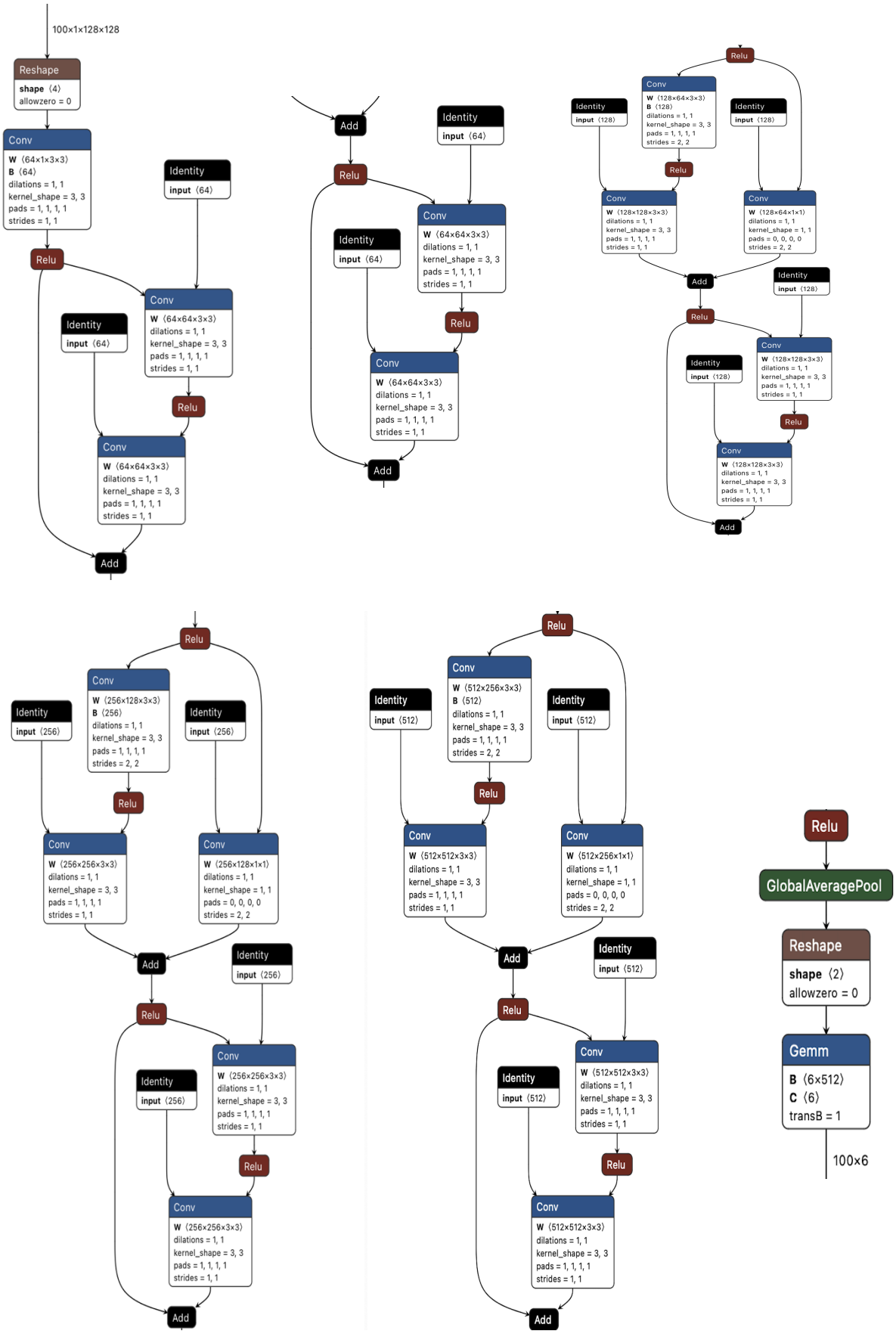

Figure: 4.3.3.1 Developing a ResNet-18 implementation tailored for training a patch-based model for multiclass classification

Chapter 5

Result and Discussion

5.1 Sagittal section 2D slices-based model outcomes

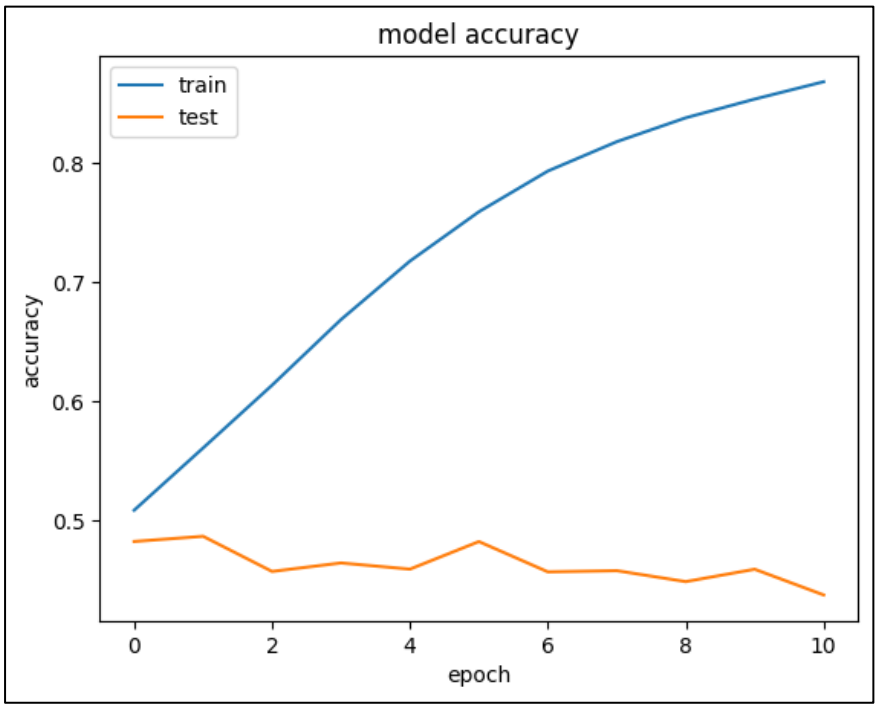

Figure:5.1.1 Model Accuracy vs Epoch of Sagittal Section

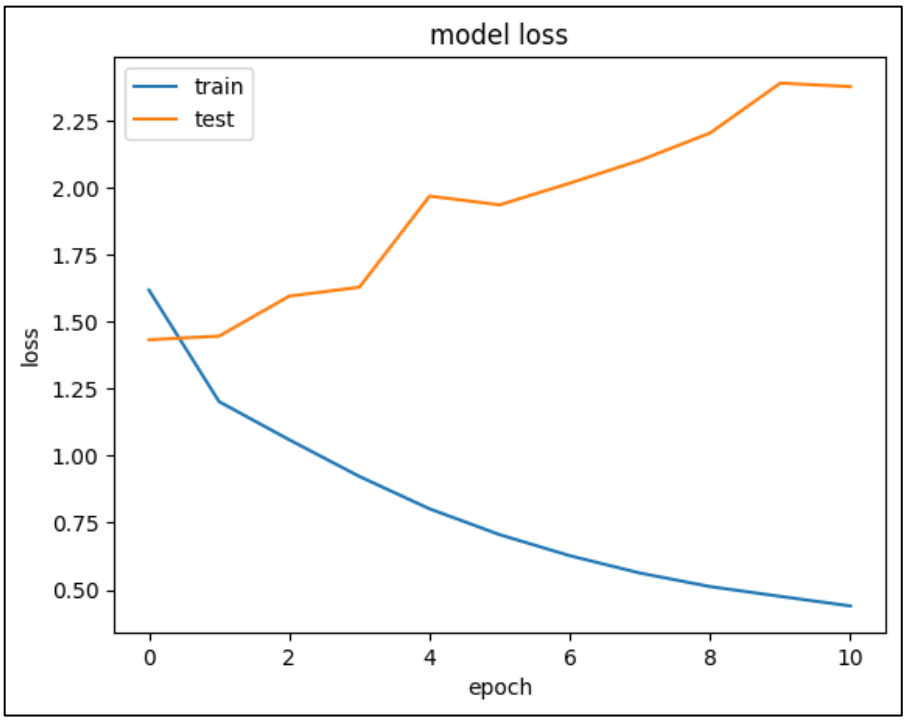

Figure:5.1.2 Model Loss of Sagittal Section

Table:5.1.1 Sagittal Section Classification Report

	Precision	Recall	F1-score	Support
AD	0.31	0.16	0.21	2250
CN	0.19	0.16	0.17	1720
EMCI	0.44	0.60	0.50	3210
LMCI	0.26	0.23	0.25	1600
MCI	0.64	0.66	0.65	4680
SMC	0.16	0.22	0.19	550
Accuracy			**0.44**	14010
Macro avg	0.33	0.34	0.33	14010
Weighted avg	0.42	0.44	0.42	14010

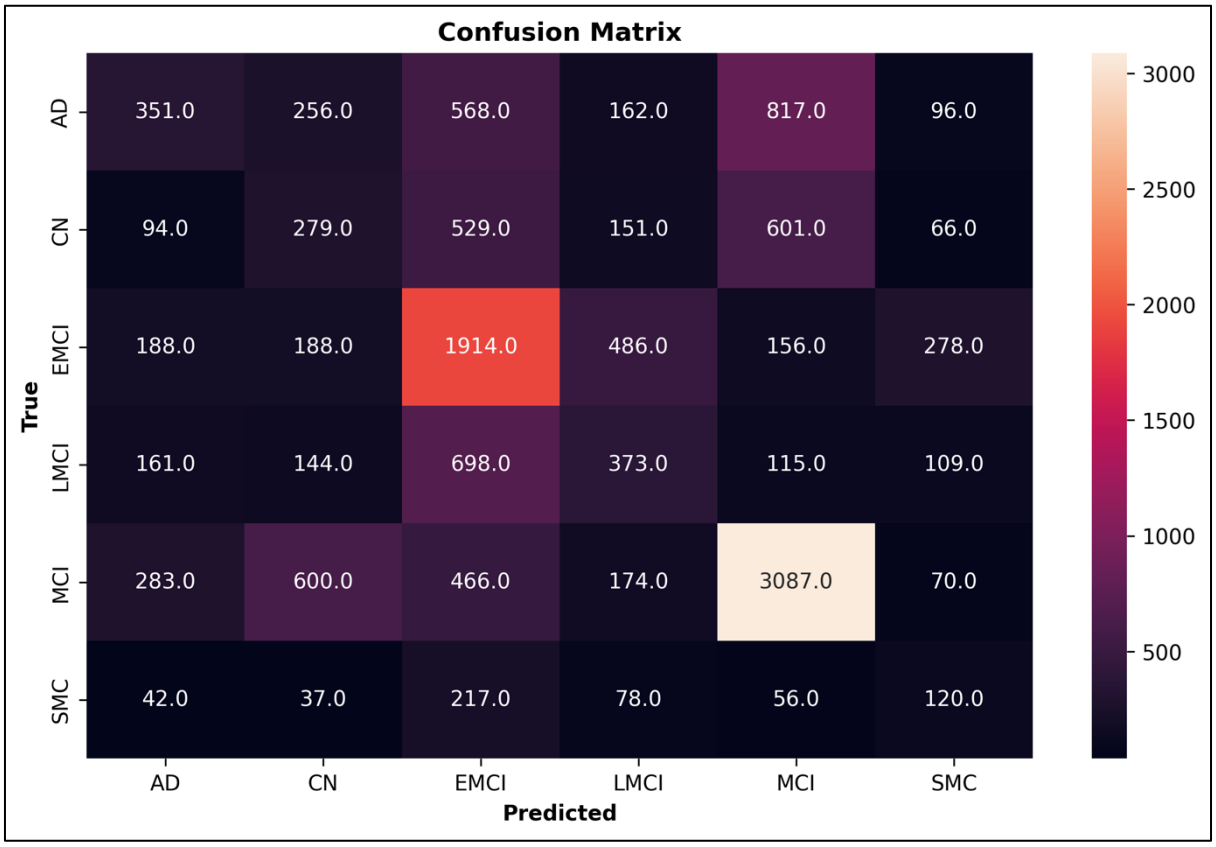

Figure:5.1.3 Sagittal Section Confusion Matrix

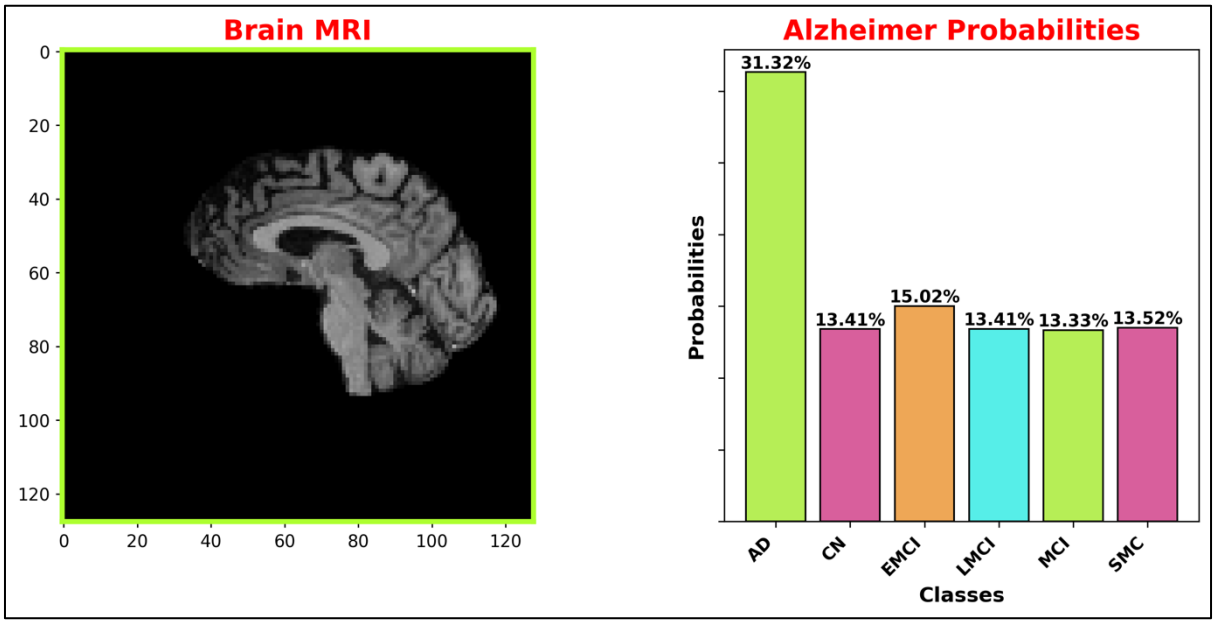

Figure:5.1.4 Prediction on test sample: The prediction result suggest that person is AD: Alzheimer Disease

5.2 Axial section 2d slices-based model outcomes

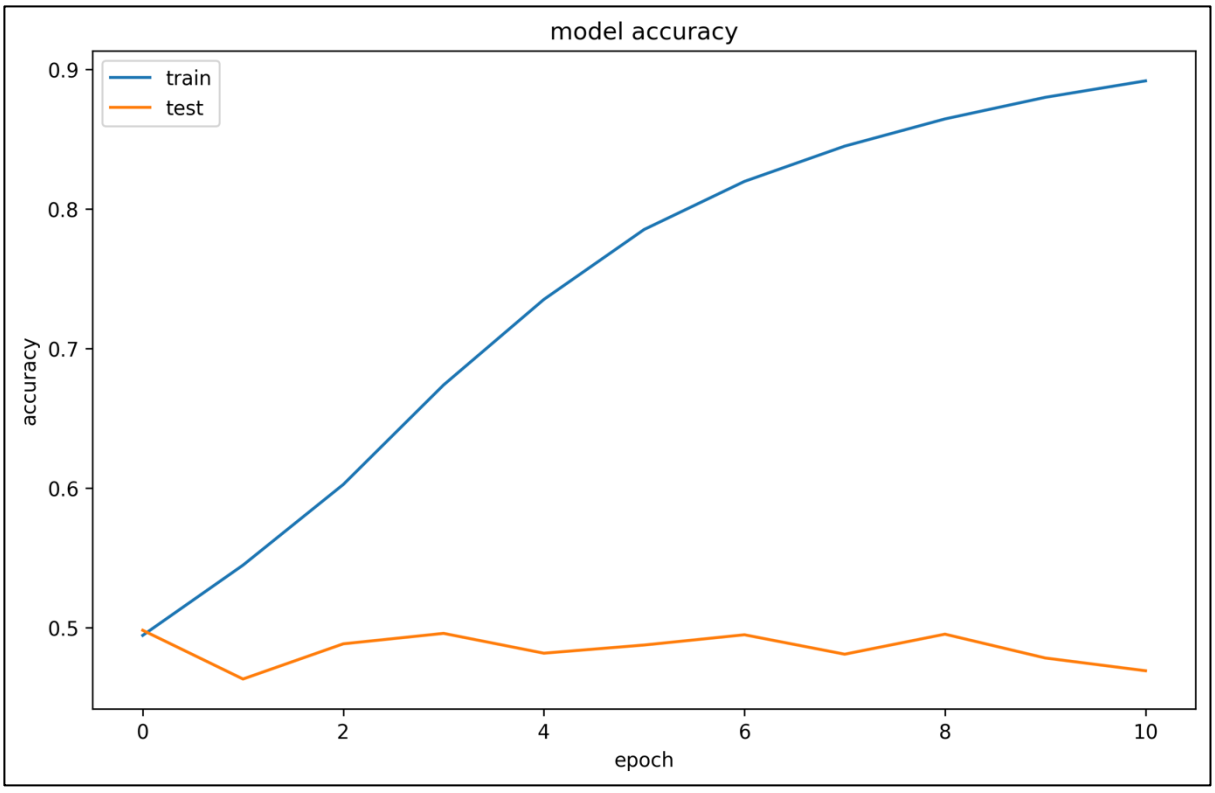

Figure:5.2.1 Model Accuracy vs Epoch of Axial Section

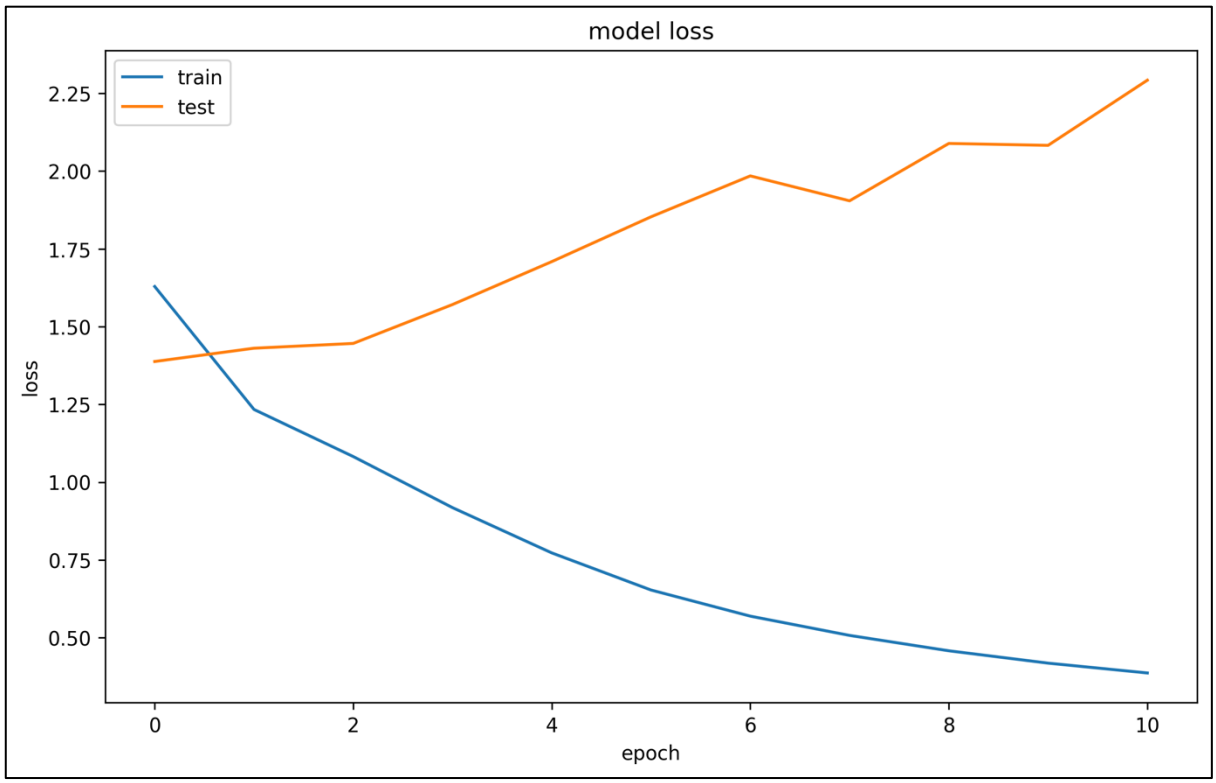

Figure:5.2.2 Model Loss of Axial Section

Table:5.2.1 Axial Section Classification Report

	Precision	Recall	F1-score	Support
AD	0.34	0.34	0.34	2250
CN	0.23	0.22	0.22	1720
EMCI	0.51	0.60	0.55	3210
LMCI	0.28	0.17	0.21	1600
MCI	0.69	0.66	0.67	4680
SMC	0.19	0.29	0.23	550
Accuracy			**0.47**	14010
Macro avg	0.37	0.38	0.37	14010
Weighted avg	0.47	0.47	0.47	14010

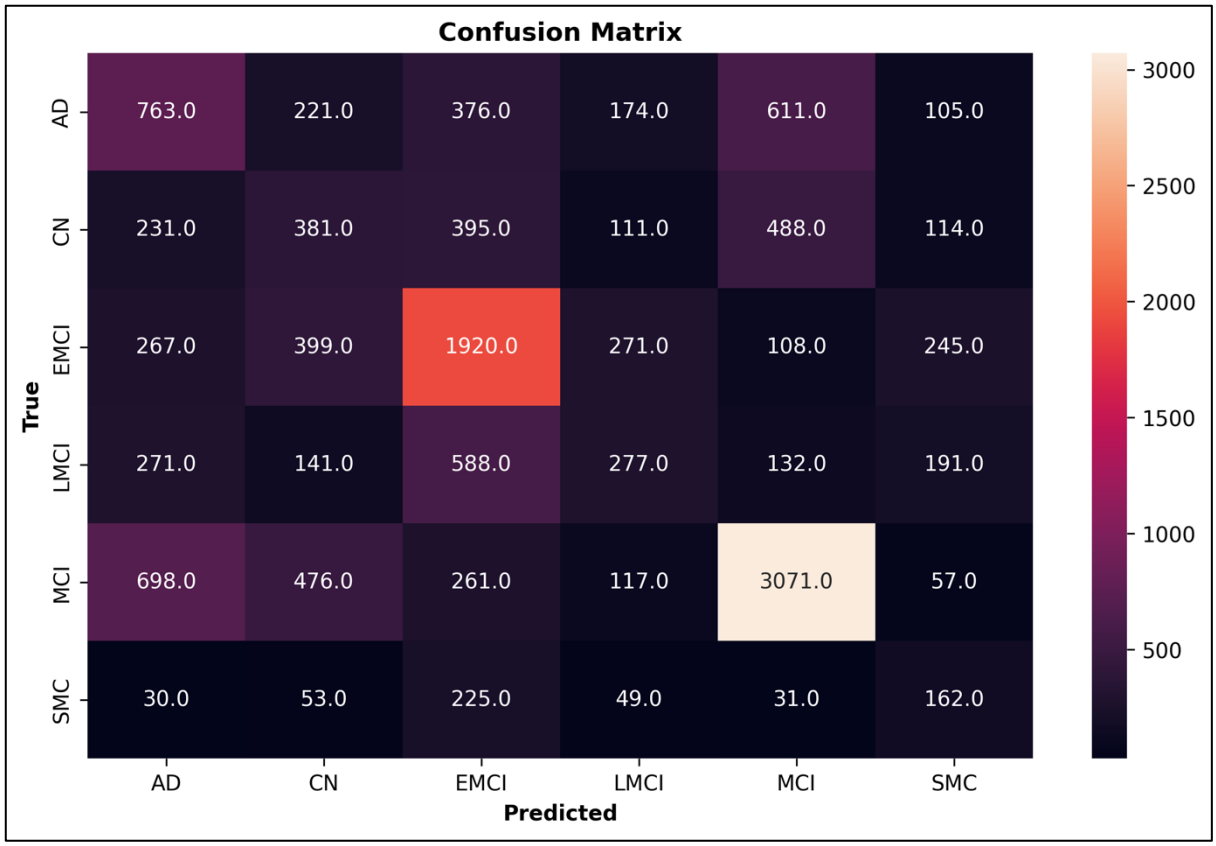

Figure:5.2.3 Confusion Matrix of Axial Section

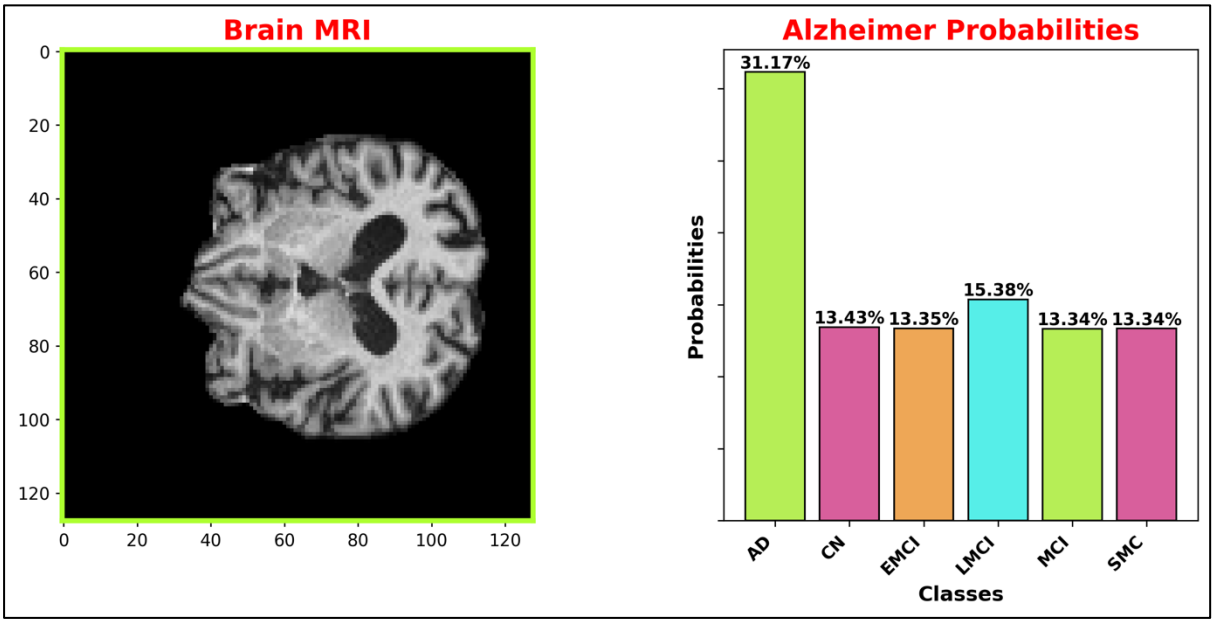

Figure:5.2.4 Prediction on test sample: The prediction result suggest that person is suffering from AD: Alzheimer Disease

5.3 Coronal section 2d slices-based model outcomes

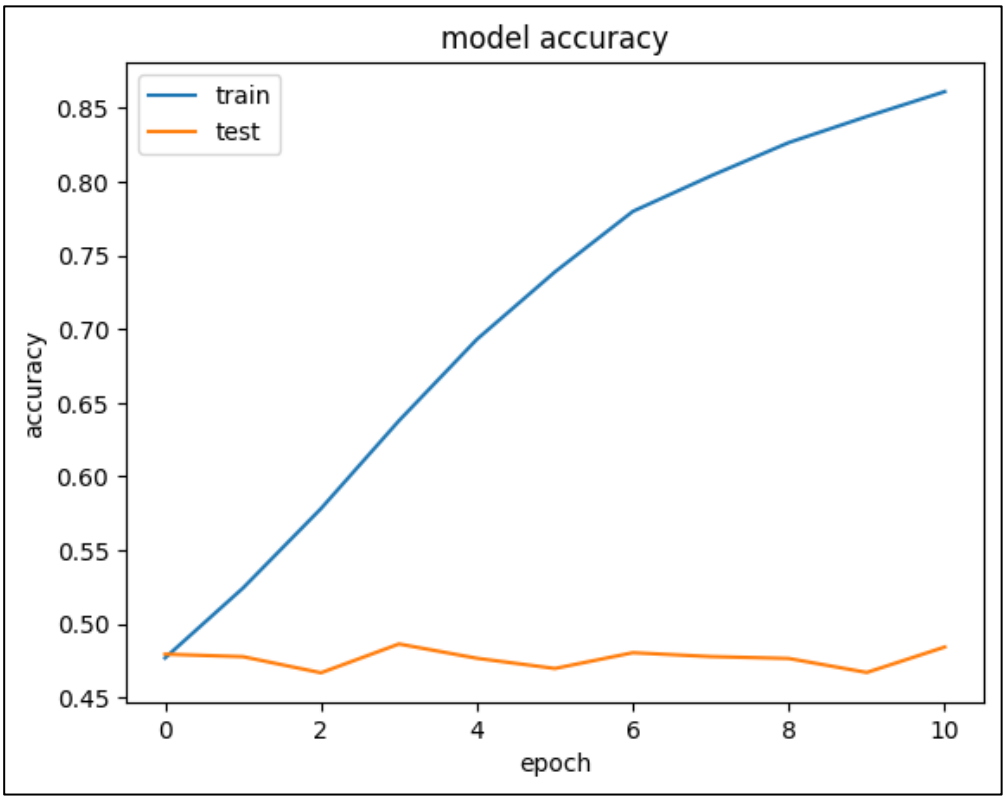

Figure:5.3.1 Model Accuracy vs Epoch of Coronal Section

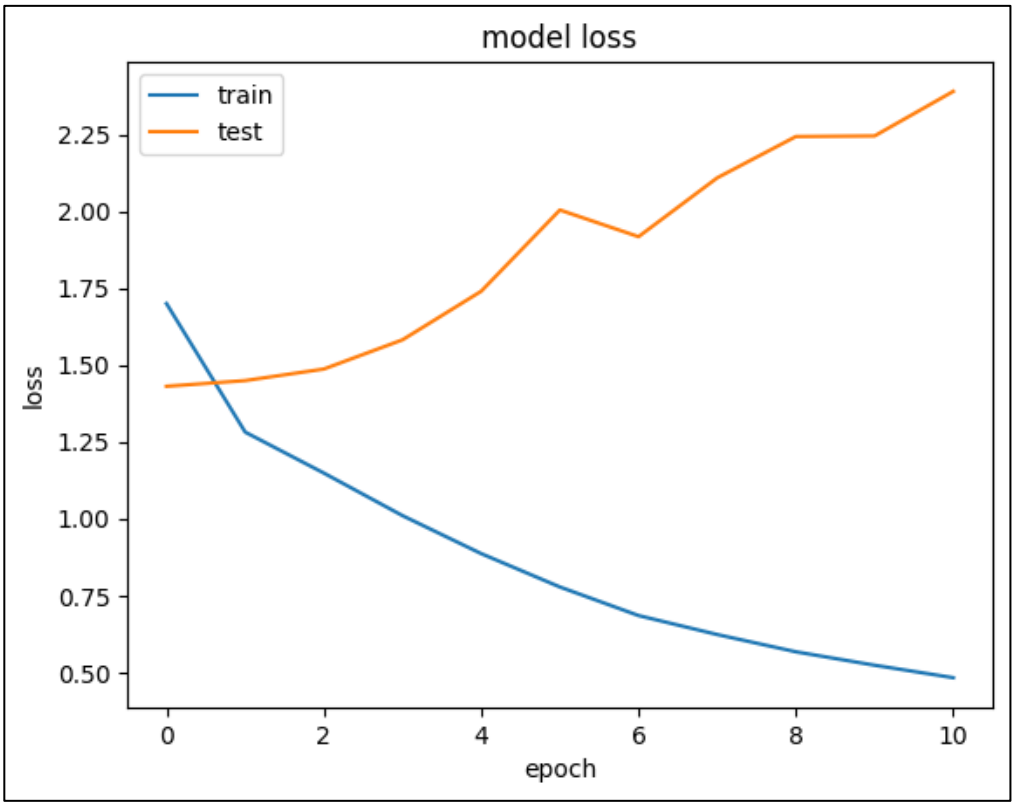

Figure:5.3.2 Model Loss of Coronal Section

Table:5.3.1 Coronal Section Classification Report

	Precision	Recall	F1-score	Support
AD	0.37	0.24	0.29	2250
CN	0.22	0.16	0.18	1720
EMCI	0.47	0.65	0.54	3210
LMCI	0.32	0.27	0.29	1600
MCI	0.67	0.71	0.69	4680
SMC	0.26	0.25	0.25	550
Accuracy			**0.48**	14010
Macro avg	0.38	0.38	0.38	14010
Weighted avg	0.46	0.48	0.47	14010

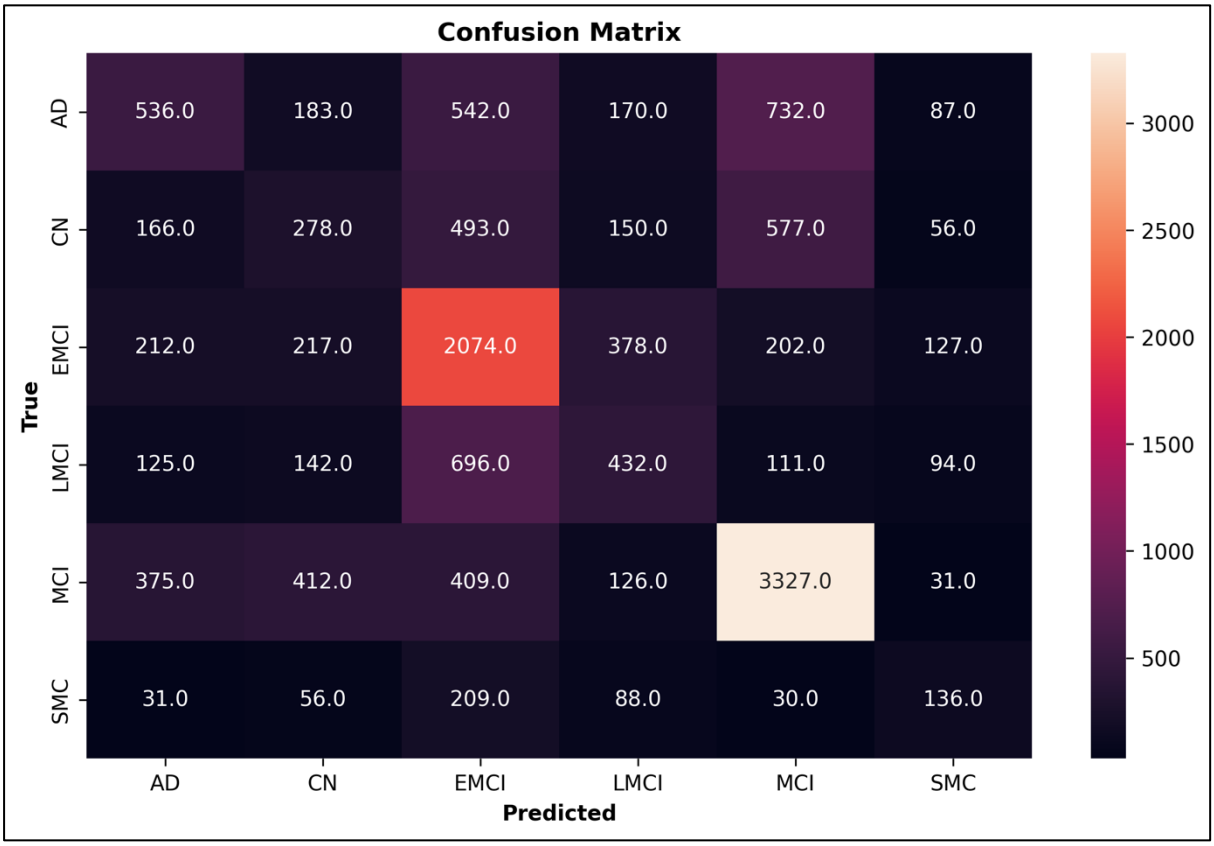

Figure:5.3.3. Confusion Matrix of Coronal Section

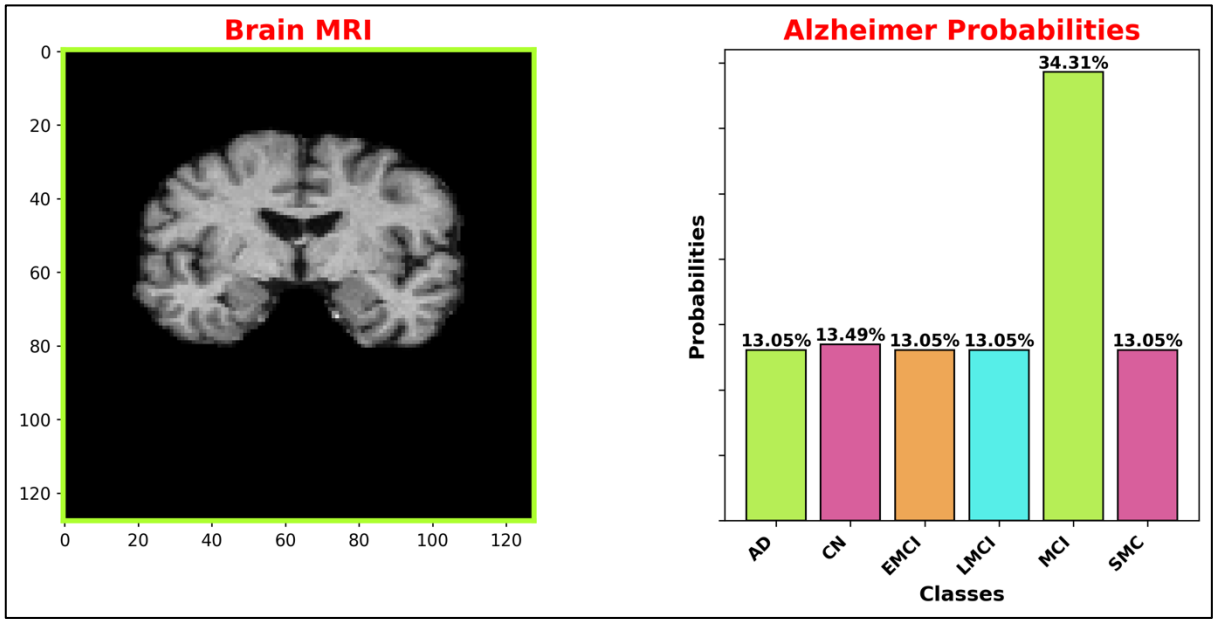

Figure: 5.3.4 Prediction on test sample: The prediction result suggest that person is suffering from Mild Cognitive Impairment

Table:5.3.1 Performance Evaluation Matrix Across Three Brain MRI Sections for Validation of 2D CNN Model

	Accuracy	macro avg Precision	weighted avg Precision	macro avg Recall	weighted avg Recall	macro avg F1-score	weighted avg F1-score
Sagittal Section	44%	33%	42%	34%	44%	33%	42%
Axial Section	47%	37%	**47%**	38%	47%	37%	47%
Coronal Sectional	**48%**	**38%**	46%	**38%**	**48%**	**38%**	**47%**

5.4 3D CNN-based Model Outcomes

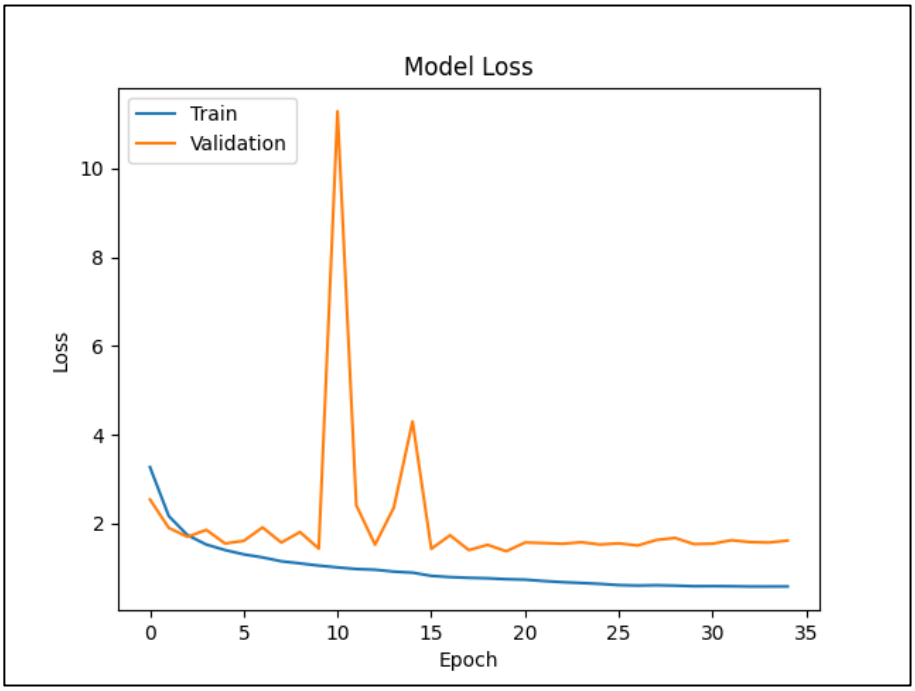

Figure:5.4.1 Model loss vs Epoch of 3D MRI

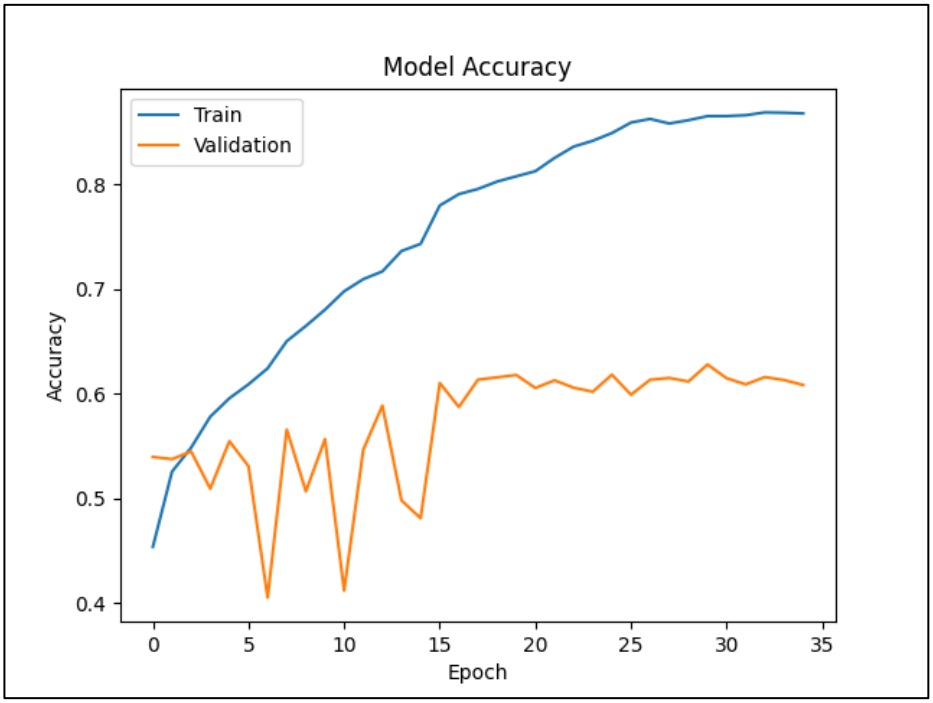

Figure:5.4.2 Model Accuracy vs Epoch of 3D MRI

By the 35th epoch, the 3D Convolutional Neural Network (CNN) model attained a classification accuracy of 0.60, corresponding to 60%, in its task of classifying Alzheimer's disease.

5.5 Patch-Based Convolutional Neural Networks

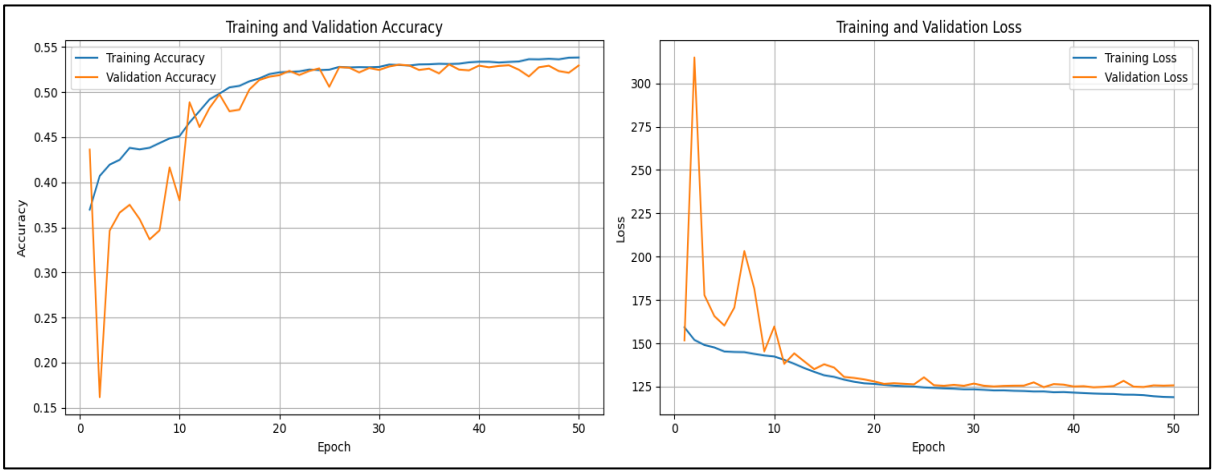

Figure:5.5.1 Patch Based Model Training and Validation Accuracy and Loss

Table:5.5.1 Patch-Based Convolutional Neural Networks Classification Report

	Precision	**Recall**	**F1-score**	**Support**
AD	0.25	0.02	0.03	22500
CN	0.01	0.00	0.00	17200
EMCI	0.44	0.92	0.59	32100
LMCI	0.30	0.02	0.04	16000
MCI	0.63	0.94	0.75	46800
SMC	0.00	0.00	0.00	5500
Accuracy			**0.53**	140100
Macro avg	0.27	0.32	0.24	140100
Weighted avg	0.39	0.53	0.40	140100

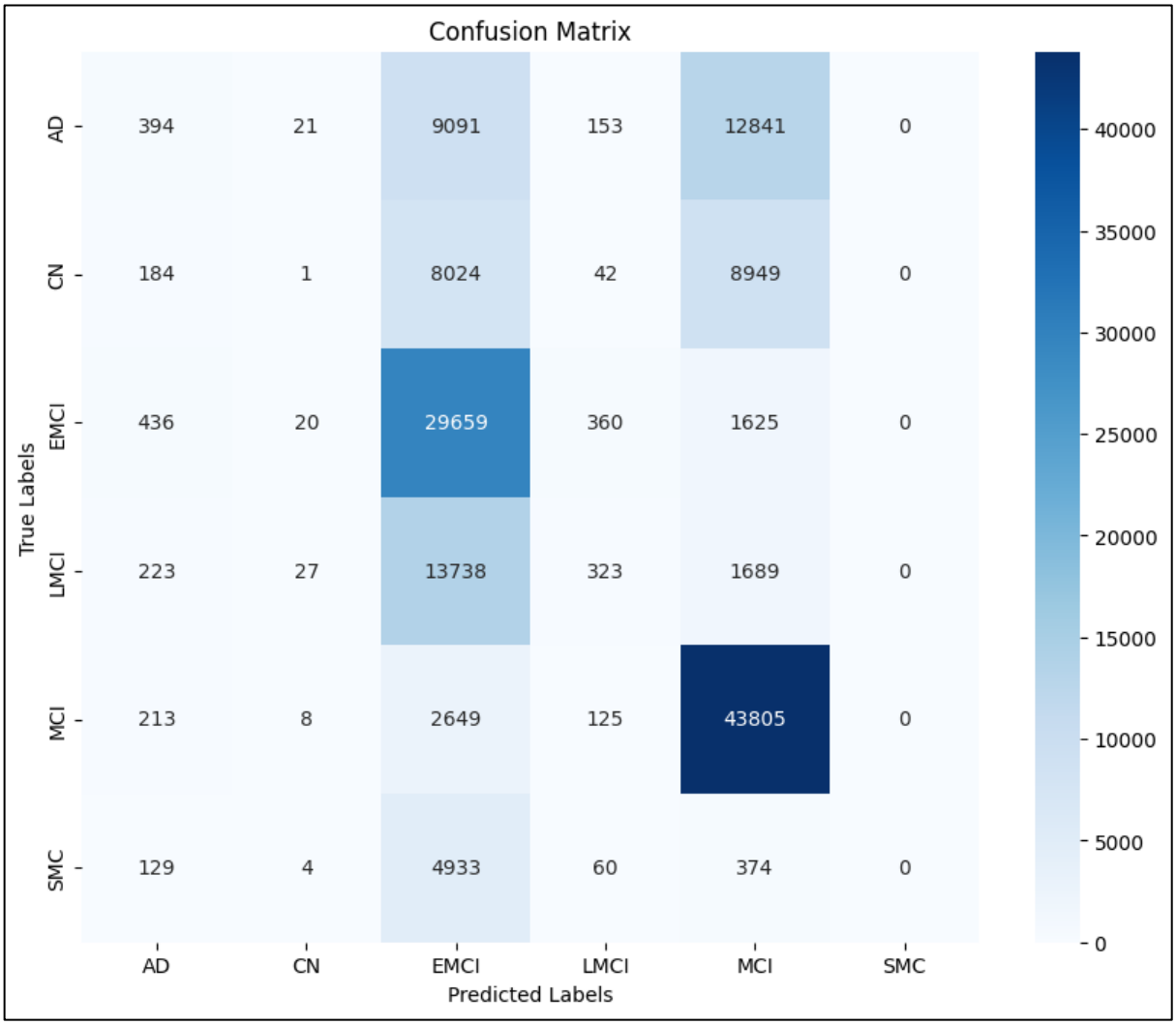

Figure:5.5.2 Patch-Based Convolutional Neural Networks Model Confusion Matrix

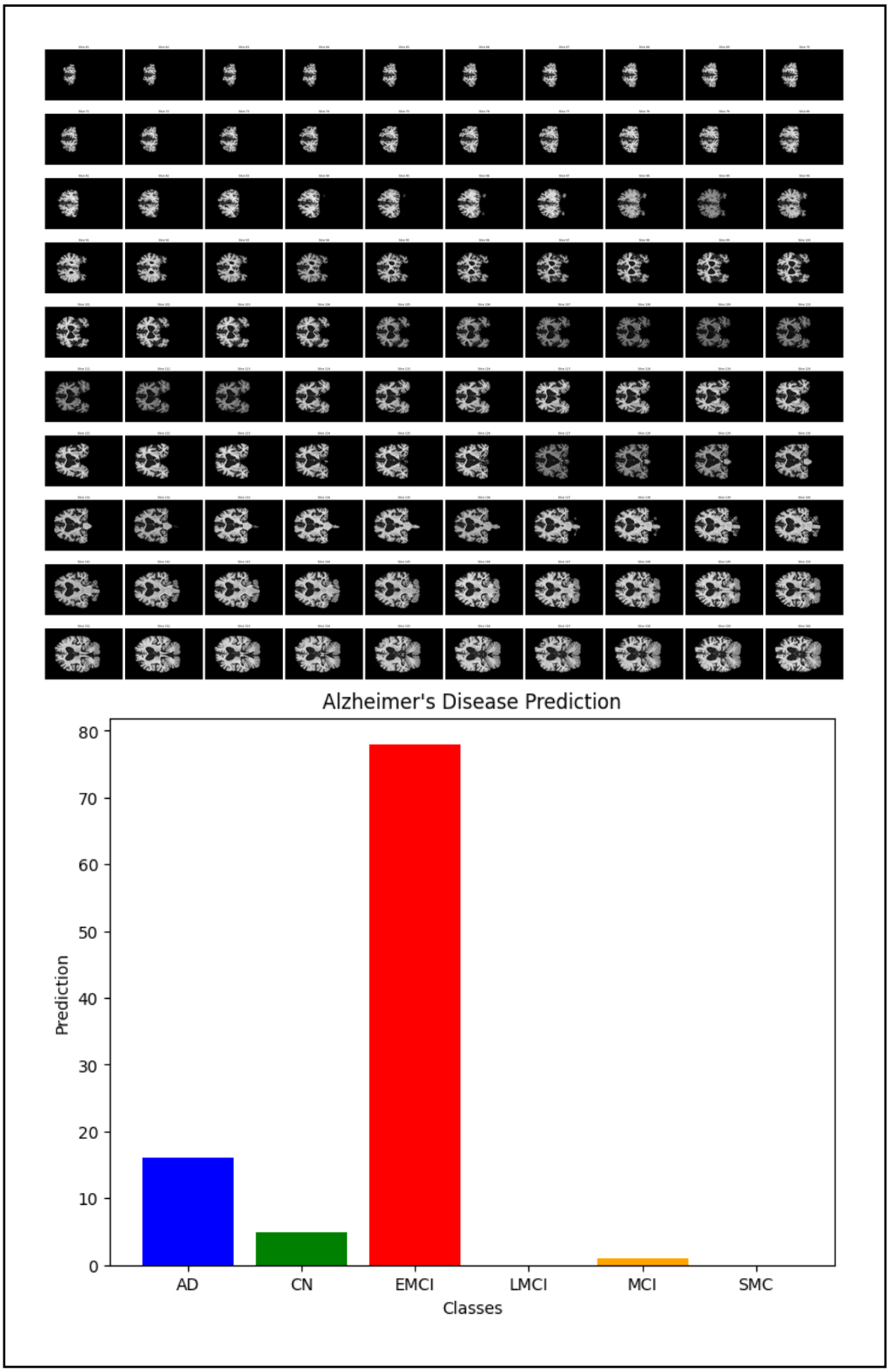

Figure:5.5.3 Prediction on test sample: The prediction result suggest that person is suffering from Early Mild Cognitive Impairment (EMCI)

5.7 Discussion

In the pursuit of accurately categorizing Alzheimer's disease (AD) through MRI data analysis, various methodologies have undergone scrutiny. Among these, the 3D CNN model has demonstrated the best performance, capturing the intricate spatial relationships and variations characteristic of AD brains by encompassing the entire MRI volume. The patch-based model follows as the second most effective method. Interestingly, within the 2D CNN approaches, the coronal section-based model has shown notable effectiveness, contrary to initial expectations that 2D methods would generally underperform compared to 3D approaches. This finding underscores the importance of meticulous slice selection and analysis, as well as the need for comprehensive exploration of diverse methodologies. The success of the coronal sections within the 2D CNN framework challenges previous assumptions and highlights the nuanced nature of MRI data analysis. This discovery emphasizes the continual reassessment and refinement of approaches to enhance accuracy in AD diagnosis and intervention. In this dynamic research landscape, remaining receptive to unexpected findings and adapting methodologies accordingly are crucial steps toward the ultimate goal of accurately classifying AD using MRI data.

5.8 Future Scope

Addressing the challenges encountered opens avenues for future research and improvement:

1. **Advanced Architectures**: Investigate novel CNN architectures tailored for MRI data analysis. Architectures like attention mechanisms or graph CNNs could better capture spatial dependencies and improve classification accuracy.
2. **Multi-Modal Fusion**: Integrate multiple imaging modalities (e.g., PET scans, fMRI) and non-imaging biomarkers (e.g., genetic markers, clinical data) for a comprehensive understanding of AD. Fusion techniques can exploit complementary information to enhance classification performance.
3. **Transfer Learning**: Pre-train models on large-scale datasets before fine-tuning on AD-specific data. Transfer learning leverages knowledge from related tasks to improve model convergence and generalization.
4. **Data Quality and Diversity**: Curate diverse and high-quality datasets encompassing various demographics, disease stages, and imaging protocols. Collaborative efforts to collect annotated datasets can facilitate robust model training and evaluation.
5. **Explainability and Interpretability**: Develop methods to interpret model decisions and highlight regions contributing to classification. Explainable AI techniques can enhance model transparency and aid clinicians in understanding and trusting automated diagnoses.

Chapter 6

Conclusion

In conclusion, this research suggests that increasing model complexity does not always yield superior results. For instance, while the 2D slice model employed a custom architecture, it did not achieve the expected performance compared to other models. Despite the initial assumption that the 3D CNN and patch-based models using the ResNet-18 architecture would offer improvements, the best performance was actually observed with the 3D CNN approach. This indicates that focusing on the 3D CNN model, which incorporates all available slices of the data rather than leaving any blank, may lead to better outcomes.

References

1. J. J. Prado and I. Rojas, "Machine Learning for Diagnosis of Alzheimer's Disease and Early Stages," *BioMedInformatics*, vol. 1, no. 3, pp. 182–200, Dec. 2021, doi: 10.3390/biomedinformatics1030012.
2. M. J. Rosenbloom and A. Pfefferbaum, "Magnetic resonance imaging of the living brain: evidence for brain degeneration among alcoholics and recovery with abstinence," *Alcohol Res Health*, vol. 31, no. 4, pp. 362–376, 2008.
3. C. Yen, C.-L. Lin, and M.-C. Chiang, "Exploring the Frontiers of Neuroimaging: A Review of Recent Advances in Understanding Brain Functioning and Disorders," *Life*, vol. 13, no. 7, p. 1472, Jun. 2023, doi: 10.3390/life13071472.
4. D. Kawahara and Y. Nagata, "T1-weighted and T2-weighted MRI image synthesis with convolutional generative adversarial networks," *Rep Pract Oncol Radiother.*, vol. 26, no. 1, pp. 35–42, Feb. 2021, doi: 10.5603/RPOR.a2021.0005.
5. M. Zaabi, N. Smaoui, H. Derbel, and W. Hariri, "Alzheimer's disease detection using convolutional neural networks and transfer learning based methods," in *2020 17th International Multi-Conference on Systems, Signals & Devices (SSD)*, Monastir, Tunisia: IEEE, Jul. 2020, pp. 939–943. doi: 10.1109/SSD49366.2020.9364155.
6. W. Al Shehri, "Alzheimer's disease diagnosis and classification using deep learning techniques," *PeerJ Computer Science*, vol. 8, p. e1177, Dec. 2022, doi: 10.7717/peerj-cs.1177.
7. M. G. Alsubaie, S. Luo, and K. Shaukat, "Alzheimer's Disease Detection Using Deep Learning on Neuroimaging: A Systematic Review," *MAKE*, vol. 6, no. 1, pp. 464–505, Feb. 2024, doi: 10.3390/make6010024.
8. J. Giorgio, S. M. Landau, W. J. Jagust, P. Tino, and Z. Kourtzi, "Modelling prognostic trajectories of cognitive decline due to Alzheimer's disease," *NeuroImage: Clinical*, vol. 26, p. 102199, 2020, doi: 10.1016/j.nicl.2020.102199.
9. S. Alp *et al.*, "Joint transformer architecture in brain 3D MRI classification: its application in Alzheimer's disease classification," *Sci Rep*, vol. 14, no. 1, p. 8996, Apr. 2024, doi: 10.1038/s41598-024-59578-3.
10. V. S. Diogo, H. A. Ferreira, D. Prata, and for the Alzheimer's Disease Neuroimaging Initiative, "Early diagnosis of Alzheimer's disease using machine learning: a multi-diagnostic, generalizable approach," *Alz Res Therapy*, vol. 14, no. 1, p. 107, Dec. 2022, doi: 10.1186/s13195-022-01047-y.
11. for the Alzheimer's Disease Neuroimaging Initiative, A. Marcisz, and J. Polanska, "Can T1-Weighted Magnetic Resonance Imaging Significantly Improve Mini-Mental State Examination-Based Distinguishing Between Mild Cognitive Impairment and Early-Stage Alzheimer's Disease?," *JAD*, vol. 92, no. 3, pp. 941–957, Apr. 2023, doi: 10.3233/JAD-220806.
12. J. B. Bae *et al.*, "Identification of Alzheimer's disease using a convolutional neural network model based on T1-weighted magnetic resonance imaging," *Sci Rep*, vol. 10, no. 1, p. 22252, Dec. 2020, doi: 10.1038/s41598-020-79243-9.
13. R. C. Petersen *et al.*, "Alzheimer's Disease Neuroimaging Initiative (ADNI): Clinical characterization," *Neurology*, vol. 74, no. 3, pp. 201–209, Jan. 2010, doi: 10.1212/WNL.0b013e3181cb3e25.
14. N. J. Tustison *et al.*, "The ANTsX ecosystem for quantitative biological and medical imaging," *Sci Rep*, vol. 11, no. 1, p. 9068, Apr. 2021, doi: 10.1038/s41598-021-87564-6.
15. IMAIOS, A. Micheau, and D. Hoa, "MRI brain: Anatomy of the brain (MRI) - cross-sectional atlas of human anatomy." IMAIOS, p. 23462, Aug. 25, 2008. doi: 10.37019/e-anatomy/163.
16. IMAIOS, A. Micheau, and D. Hoa, "MRI axial brain: Anatomy of the encephalon (MRI) in axial slices." IMAIOS, p. 23555, Sep. 09, 2009. doi: 10.37019/e-anatomy/49541.
17. V. Nair and G. E. Hinton, "Rectified linear units improve restricted boltzmann machines," in *ICML 2010*, 2010, pp. 807--814.
18. K. He, X. Zhang, S. Ren, and J. Sun, "Delving Deep into Rectifiers: Surpassing Human-Level Performance on ImageNet Classification," 2015, doi: 10.48550/ARXIV.1502.01852.
19. K. He, X. Zhang, S. Ren, and J. Sun, "Deep Residual Learning for Image Recognition." arXiv, Dec. 10, 2015. Accessed: May 14, 2024. [Online]. Available: http://arxiv.org/abs/1512.03385